

Synthesis and Biological Evaluation of Manassantin Analogues for Hypoxia-Inducible Factor 1 α Inhibition

Do-Yeon Kwon,^{†,‡} Hye Eun Lee,^{‡,§} Douglas H. Weitzel,[§] Kyunghye Park,[‡] Sun Hee Lee,[‡] Chen-Ting Lee,[§] Tesia N. Stephenson,[†] Hyeri Park,[†] Michael C. Fitzgerald,[†] Jen-Tsan Chi,[¶] Robert A. Mook, Jr.,^{||} Mark W. Dewhirst,[§] You Mie Lee,^{*,‡} and Jiyong Hong^{*,†,⊥}

[†]Department of Chemistry, Duke University, Durham, North Carolina 27708, United States

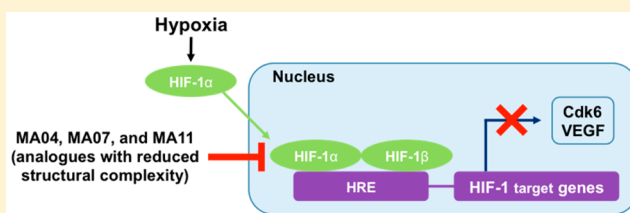
[‡]College of Pharmacy, Research Institute of Pharmaceutical Sciences, Kyungpook National University, 80 Daehak-ro, Buk-gu, 702-701 Daegu, Republic of Korea

[§]Department of Radiation Oncology, [¶]Department of Molecular Genetics & Microbiology, ^{||}Department of Medicine, and

[⊥]Department of Pharmacology and Cancer Biology, Duke University Medical Center, Durham, North Carolina 27710, United States

Supporting Information

ABSTRACT: To cope with hypoxia, tumor cells have developed a number of adaptive mechanisms mediated by hypoxia-inducible factor 1 (HIF-1) to promote angiogenesis and cell survival. Due to significant roles of HIF-1 in the initiation, progression, metastasis, and resistance to treatment of most solid tumors, a considerable amount of effort has been made to identify HIF-1 inhibitors for treatment of cancer. Isolated from *Saururus cernuus*, manassantins A (1) and B (2) are potent inhibitors of HIF-1 activity. To define the structural requirements of manassantins for HIF-1 inhibition, we prepared and evaluated a series of manassantin analogues. Our SAR studies examined key regions of manassantin's structure in order to understand the impact of these regions on biological activity and to define modifications that can lead to improved performance and drug-like properties. Our efforts identified several manassantin analogues with reduced structural complexity as potential lead compounds for further development. Analogues MA04, MA07, and MA11 down-regulated hypoxia-induced expression of the HIF-1 α protein and reduced the levels of HIF-1 target genes, including cyclin-dependent kinase 6 (Cdk6) and vascular endothelial growth factor (VEGF). These findings provide an important framework to design potent and selective HIF-1 α inhibitors, which is necessary to aid translation of manassantin-derived natural products to the clinic as novel therapeutics for cancers.



INTRODUCTION

Molecular oxygen (O₂) is required for aerobic metabolism to maintain intracellular bioenergetics and serves as an electron acceptor in many biochemical reactions.¹ Ambient air contains 21% of O₂; however, most mammalian tissues exist at 2–9% O₂. Hypoxia, usually defined as $\leq 2\%$ O₂, occurs in a variety of pathological conditions, including stroke, tissue ischemia, inflammation, and tumor growth.² Cells have developed a number of essential mechanisms to cope with the stress of hypoxia. Among these coping mechanisms is the response mediated by the hypoxia-inducible factor 1 (HIF-1).³

HIF-1 is a basic helix–loop–helix PER-ARNT-SIM (bHLH-PAS) family protein that forms a heterodimer with its α and β subunits and functions as a transcription factor.⁴ While HIF-1 β is constitutively active, HIF-1 α is regulated by oxygen status. In well-oxygenated states, constitutively synthesized HIF-1 α undergoes continuous degradation.⁵ During this process, two proline sites (Pro402 and Pro564) in the oxygen-dependent degradation (ODD) domain are hydroxylated by prolyl hydroxylase.⁶ Of the three prolyl hydroxylases (PHD1, PHD2, and PHD3) identified in mammalian cells, PHD2 is

known to play a major role. Under normoxic conditions, PHD2 uses molecular oxygen and 2-oxoglutarate (α -ketoglutarate) as cosubstrates for proline hydroxylation of HIF-1 α . Hydroxylated HIF-1 α is then recognized by the tumor suppressor protein von Hippel–Lindau (VHL), subsequently ubiquitinated, and degraded. Hypoxic O₂ levels limit the ability of PHD2 to function and result in enhanced stability of HIF-1 α . Stabilized HIF-1 α forms a heterodimer with its β subunit and translocates into the nucleus where it binds to its target gene promoters known as hypoxia response elements (HREs) and activates gene transcription. HIF-1 is a main regulator of hypoxia, activating several hundred genes involved in angiogenesis (VEGF), glucose transport (GLUT1), glycolytic pathways (LDH-A), ROS signals (iNOS), erythropoiesis (EPO), and a variety of other processes.⁷

Tumors adapt to hypoxia by increasing angiogenesis and metastatic potential, altering apoptosis, and regulating metabolism.⁸ These adaptations mediated by HIF-1 make tumors

Received: March 10, 2015

Published: September 22, 2015

both more aggressive and treatment-resistant, resulting in poor clinical outcomes.^{9–11} Immunohistochemical analyses have revealed that HIF-1 α is overexpressed in many human cancers and is closely associated with patient mortality.¹² HIF-1 overexpression is not only involved in tumor progression but also associated with resistance to radiation and chemotherapy.^{13–15} Due to the importance of HIF-1 in tumor development and progression, a considerable amount of effort has been made to identify HIF-1 inhibitors for treatment of cancer.^{16–20}

Saururus cernuus L. (Saururaceae), an aquatic plant found throughout the eastern half of the United States, has a long history of medicinal use in the treatment of tumors by both native Americans and early colonists. The dineolignans manassantin A (1), manassantin B (2), 4-*O*-demethylmanassantin B (3), and manassantin B₁ (4) are natural products isolated from *Saururus cernuus* (Figure 1).^{21–23} Manassantins (1–4) have been shown to be HIF-1 inhibitors *in vitro*.^{22–24}

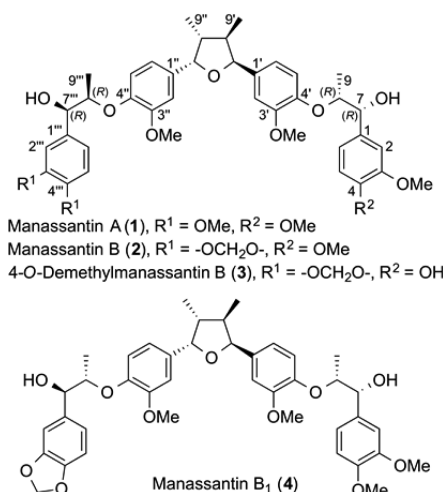


Figure 1. Structure of dineolignans from *Saururus cernuus*.

In broad connection with our interest in using natural products to understand the signaling pathways in biology,^{25–28} we devised a convergent synthetic route to 1 and 2 that would be easily amenable to the synthesis of analogues for biological studies.²⁴ After completing the synthesis of 1 and 2, we determined the effect of these manassantins on HIF-1 and VEGF expression.^{24,29} These studies revealed that manassantin A (1) is a potent inhibitor of HIF-1 activity. Western blots of 4T1 cells (murine mammary carcinoma cells) exposed to 1 under hypoxic conditions showed that hypoxia-induced HIF-1 α expression was significantly inhibited at concentrations between 10 and 100 nM. Furthermore, HIF-1 regulated VEGF secretion was dramatically reduced by 1. Evaluation of 1 in the National Cancer Institute's 60-cell line screen³⁰ showed that 1 possesses strong differential cytotoxicities against several breast, leukemia, and melanoma cell lines (see the Supporting Information for details).

Encouraged by the potential of manassantins as novel therapeutics for cancer, we prepared a series of manassantin analogues to define the structural requirements for HIF-1 inhibition. Herein, we describe our efforts toward the synthesis and SAR study of manassantin analogues to guide the design of structurally simplified manassantins for anticancer therapeutic development.

RESULTS AND DISCUSSION

Chemistry. Manassantins A (1) and B (2) consist of two regions (Figure 2): a tetrahydrofuran core region and a side

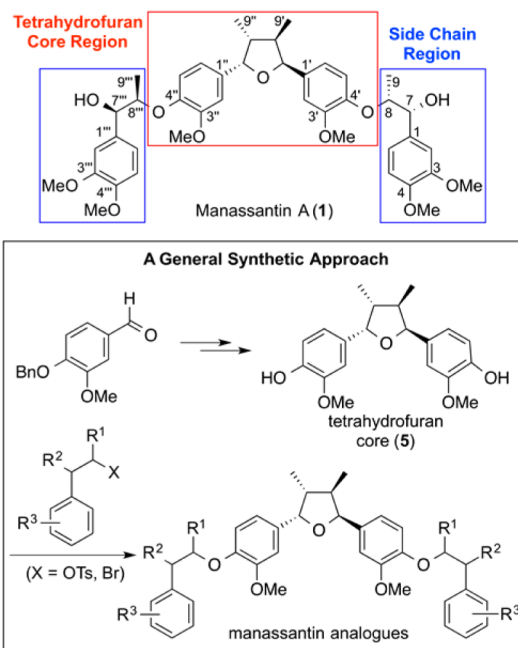


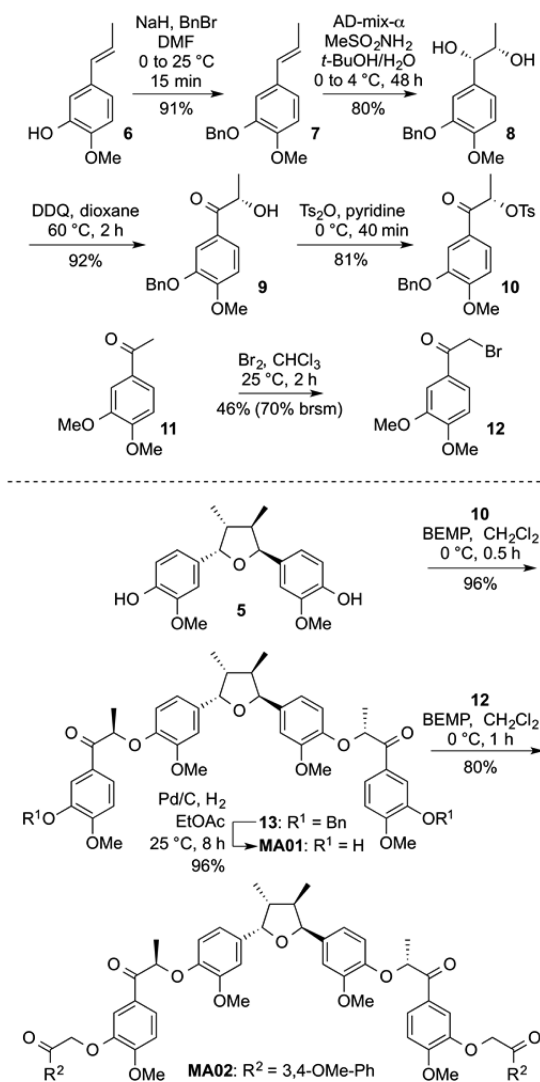
Figure 2. A convergent synthetic approach to manassantin analogues.

chain region. Since we demonstrated that the 2,3-*cis*-3,4-*trans*-4,5-*cis*-configuration of the tetrahydrofuran core is critical for HIF-1 inhibition,²⁹ we envisioned the preparation of a series of analogues with modification of the substituents and the length of the side chains in an effort to establish a more comprehensive SAR and identify manassantin analogues with reduced structural complexity. The manassantin analogues could be easily prepared from the known tetrahydrofuran core 5²⁴ following the convergent synthetic approach shown in Figure 2. We anticipated that SAR studies would identify structural motifs and minimal structural requirements required for HIF-1 inhibition. Such information will allow structural modifications to increase specificity, decrease off-target effects, and improve drug performance.

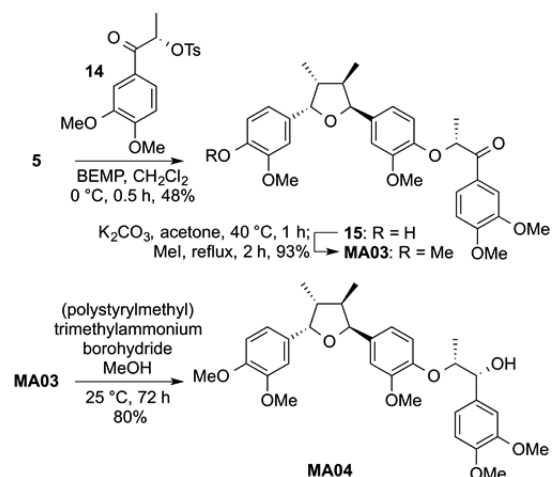
First, we prepared an extended side chain analogue (MA02) to gain insights into the importance of side chain length in HIF-1 inhibition. The synthesis of MA02 started with the preparation of tosylate 10 and α -bromoketone 12 for coupling reactions (Scheme 1). Benzyl (Bn)-protection of the known *trans-m*-propenyl guaiacol (6)³¹ followed by asymmetric dihydroxylation³² of 7 provided diol 8. Selective DDQ-oxidation of the benzylic hydroxyl group of 9 followed by tosylation successfully afforded 10. α -Bromoketone 12 was prepared by treatment of the commercially available 3',4'-dimethoxyacetophenone (11) with Br₂.³³ BEMP-mediated coupling of tetrahydrofuran core 5²⁴ and tosylate 10 and Bn-deprotection provided MA01 in excellent overall yield. Final coupling of MA01 with 12 completed the synthesis of MA02.

As shown in Scheme 2, a truncated analogue (MA03) was prepared by monoalkylation of 5 with the known tosylate 14²⁴ (48%) followed by methylation (K₂CO₃, MeI, 93%). Stereoselective reduction of MA03 with polymer-bound BH₄ afforded the desired truncated analogue (MA04, 4-*O*-methylsauer-

Scheme 1. Synthesis of Extended Analogue (MA02)



Scheme 2. Synthesis of Truncated Analogues (MA03 and MA04)

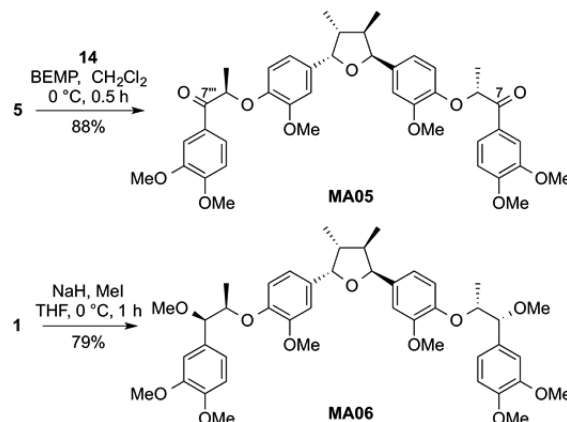


neol)²³ in 80% yield, which constitutes the first synthesis of 4-O-methylsaucerneol.

We hypothesized that the C7 and C7'' hydroxyl groups could play an important role by providing hydrogen bonds to

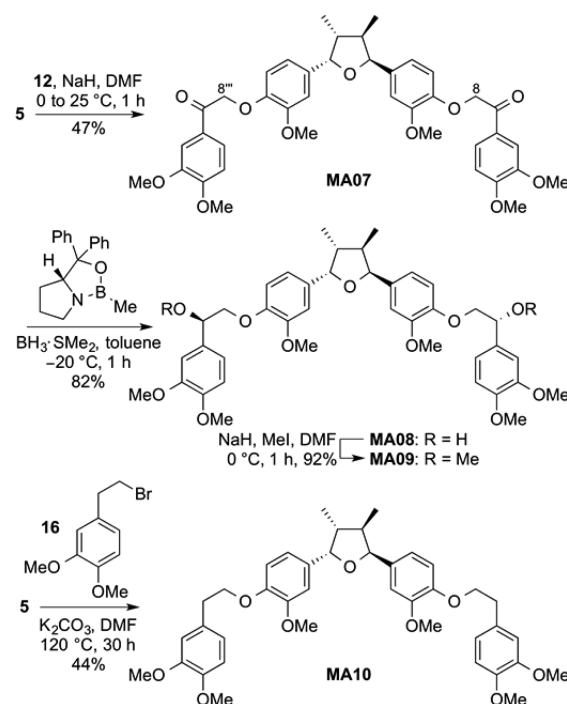
the binding target(s) or influencing the conformation of the side chains via intramolecular hydrogen bonds with the neighboring ether oxygen atom. To test this hypothesis, we synthesized the corresponding keto analogue (MA05)²⁴ by coupling 5 and 14. The C7/C7'' methoxy analogue (MA06) was prepared by methylation of manassantin A (1) with NaH and MeI (79%) (Scheme 3).

Scheme 3. Synthesis of C7/C7'' Keto and Methoxy Analogues (MA05 and MA06)



To define the role of C8/C8'' methyl groups and reduce the structural complexity of manassantin side chains, we prepared C8/C8'' desmethyl analogues (MA07–MA09) and C8/C8'' desmethyl and C7/C7'' deoxy analogue (MA10) (Scheme 4). Alkylation of tetrahydrofuran core 5 with α -bromoketone 12 provided MA07 in modest yield. Asymmetric Corey–Bakshi–Shibata reduction³⁴ of MA07 afforded MA08 as a single diastereomer (82%), which was further converted to MA09 by

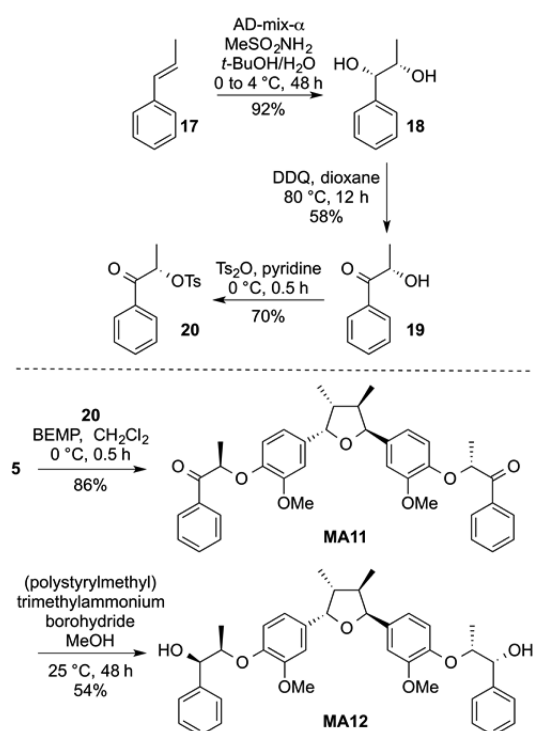
Scheme 4. Synthesis of C8/C8'' Desmethyl and C7/C7'' Deoxy Analogues (MA07–MA10)



methylation with NaH and MeI. To further reduce the complexity of manassantins, we removed both C8/C8'' methyl and C7/C7'' hydroxyl groups and prepared **MA10** by coupling **5** with the commercially available 4-(2-bromoethyl)-veratrole (**16**). In addition to reducing the structural complexity, removal of the benzylic hydroxyl groups would reduce the number of hydrogen-bonding donors and influence PK/PD parameters by improving permeability and absorption and removing the potential metabolism site (e.g., phase-2 conjugation).³⁵

Previously, it was reported that a reduction in potency was observed with the replacement of the C4 methoxy group in the distal phenyl rings of manassantins A (**1**, Figure 1) and B (**2**) with a hydroxyl group as in 4-*O*-demethylmanassantin B (**3**).²³ To characterize the role of the methoxy groups on the distal phenyl rings, we prepared the C3/C3'' hydroxy analogue (**MA01**) (the intermediate to **MA02**, Scheme 1) and phenyl analogues (**MA11** and **MA12**) (Scheme 5). Asymmetric

Scheme 5. Synthesis of Phenyl Analogues (MA11 and MA12)



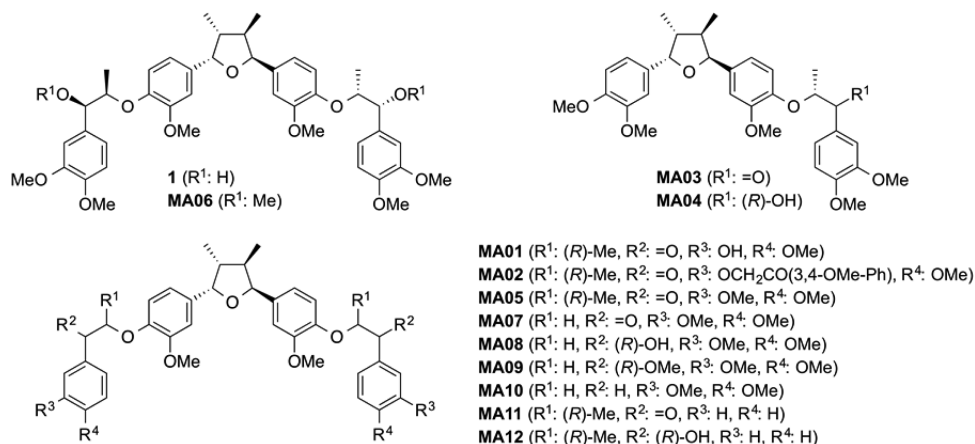
dihydroxylation of the commercially available (*E*)-1-propenylbenzene (**17**) provided diol **18** in 92% yield. Selective DDQ-oxidation of the benzylic hydroxyl group of **18** followed by tosylation smoothly proceeded to afford tosylate **20**. BEMP-mediated coupling of **5** with **20** successfully provided **MA11**, which was reduced stereoselectively to give **MA12**.

Biological Characterization. After the completion of the analogue synthesis, we performed a dual luciferase-reporter assay to assess the effect of manassantin analogues (**MA01**–**MA12**) on HIF-1 activity. We used HEK-293T cells (human embryonic kidney cells) transiently transfected with both pGL3-SHRE-Luc (pGL3-HRE-Luc) and pRL-SV40 encoding *Renilla* luciferase (pRen-Luc) vectors to investigate the effect of **MA01**–**MA12** on HIF-1 transactivation activity. We generated a reporter vector, pGL3-HRE-luciferase plasmid containing five copies of HRE sequences identical to that in the human VEGF

promoter gene. The dual luciferase-reporter assay was used as an initial *in vitro* test to identify active compounds for further evaluation. HEK-293T cells were seeded in a 96-well plate at a density of 5×10^3 cells/well. After 24 h incubation, cells were treated with hypoxic conditions (1% O₂) and serially diluted compounds (**1** and **MA01**–**MA12**) for 24 h. To measure the firefly luminescence signals, Dual-Glo reagent was added, and the luminescence signals were measured by using a dual-color luminescence detection system. The luciferase signals were normalized to the activity of *Renilla* luciferase and quantified as relative light units (RLU) (see the Supporting Information for details).

None of the analogues tested was as potent as manassantin A (**1**), but several manassantin analogues reduced the luciferase signal to the maximum percent inhibition level relative to that observed under normoxic conditions (Table 1). The luciferase assay provided several valuable insights into SAR. First, the extended analogue **MA02** was almost inactive, suggesting the importance of the side chain length of manassantins in HIF-1 inhibitory activity. The truncated analogue **MA04** (4-*O*-methylsauerneol), although less potent than **1**, still showed strong inhibition of HIF-1 activity (IC₅₀ = 0.32 μM). Previously, Zhou and co-workers reported that **MA04** is less potent than **1** due to the absence of one side chain phenylpropyl unit,²³ which was further confirmed by our study. Although **MA04** possesses lower potency relative to **1**, the reduced molecular weight, hydrophobicity, and structural complexity obtained by removing one of the two side chains of **1** may allow for improvement of other crucial parameters in drug discovery (see the Supporting Information for details).³⁵ Ligand efficiency (LE) has been utilized as a method for improving the overall performance of molecules by providing an index of how effectively a molecule uses its structural features to bind and inhibit its target.^{36,37} Ligand efficiency indices compare molecules according to their average binding energy per atom or potency of inhibition per atom. This concept has been extended to include other properties such as lipophilicity, molecular mass, and polar surface area. These measures are typically focused on *in vitro* binding affinity and not on *in vivo* properties. Since overemphasis on potency can often produce large molecules with poor drug properties, optimizing ligand efficiency can be a very important metric in lead optimization. When the LE and physicochemical properties of **MA04** were calculated using the activity in our dual luciferase-reporter assay (see the Supporting Information for details), **MA04** showed better ligand efficiency index (LEI, **MA04** = 0.16 vs **1** = 0.15) and binding efficiency index (BEI, **MA04** = 11.74 vs **1** = 10.84) than **1**. Moreover, **MA04** compared more favorably than **1** in other physicochemical property assessments (e.g., cLogP, number of rotatable bonds). Although multiple parameters (e.g., cell permeability) can impact cellular activity such that theoretical considerations of LE may not be directly applicable, the potency of **MA04** is significant given the improvement in many other parameters associated with good drug properties.

Analogues with the C7/C7'' keto groups (**MA03** and **MA05**) showed lower activities than analogues with hydroxyl groups at the same positions (**MA03** vs **MA04**, **MA05** vs **1**), suggesting that the C7/C7'' hydroxyl groups are important to the potency of **1**. Methylation of the C7/C7'' hydroxyl groups (**MA06** and **MA09**) also reduced the potency (**MA06** vs **1**, **MA09** vs **MA08**). Removal of the C9/C9'' methyl groups lowered the activity of the analogues (**MA08** vs **1**, **MA09** vs

Table 1. Chemical Structures and IC₅₀ Values of MA01–MA12 in Dual Luciferase-Reporter Assay

compound	IC ₅₀ ^a (μM)	maximum percent inhibition relative to normoxia ^a (%)
manassantin A (1)	0.011 ± 0.003	103 ± 11
MA01	2.11 ± 0.66	78 ± 6
MA02	>10,000	36 ± 12
MA03	3.70 ± 0.37	82 ± 6
MA04	0.32 ± 0.10	113 ± 1
MA05	0.91 ± 0.27	114 ± 5
MA06	0.43 ± 0.14	102 ± 12
MA07	0.35 ± 0.05	93 ± 10
MA08	0.38 ± 0.10	94 ± 4
MA09	1.93 ± 0.70	87 ± 8
MA10	1.44 ± 0.62	64 ± 7
MA11	0.69 ± 0.39	101 ± 18
MA12	0.59 ± 0.12	79 ± 5

^aData are mean values of three independent experiments. Errors represent standard deviation.

MA06), although in the C7/C7^m keto analogues, **MA07** demonstrated good activity (IC₅₀ = 0.35 μM) compared with **MA05** (IC₅₀ = 0.91 μM). The lack of the C9/C9^m methyl groups and displacement of the C7/C7^m hydroxyl groups with keto groups in the structure of **MA07** dramatically simplifies the chemistry. Analogues (**MA11** and **MA12**) without the methoxy groups in the distal phenyl rings were significantly less potent than **1**, however, they showed IC₅₀ values in the submicromolar range. Given that methoxy groups in a phenyl ring can be metabolically labile,³⁸ this result is noteworthy because it provides SAR information to guide optimization of PK parameters and to help design affinity probes for target identification studies.

One of the most critical aspects of drug discovery programs driven by natural products is the identification of structurally simple and synthetically more accessible compounds,³⁹ which ultimately aids the preparation of compounds in large quantities for preclinical and clinical studies. None of the analogues that we prepared and tested was as potent as **1**, but several analogues with reduced structural complexity such as **MA04** warrant further biological evaluations in this regard.

General toxicity of manassantin analogues was examined using the MTT assay, a standard colorimetric cytotoxicity assay. HEK-293T cells were seeded in a 96-well plate and treated with serially diluted **1** and **MA01–MA12** (0.005–10 μM) for 24 h under hypoxia. After 24 h treatment, MTT was added following manufacturer's protocol. The absorbance of the formazan was detected at 540 nm. Up to the highest concentration examined (10 μM), cells had >80% survival rate in HEK-293T (see the Supporting Information for details).

Following the initial dual luciferase-reporter assay, we used Western blots to further examine the down-regulation of HIF-1α by manassantin analogues. We selected a subset of manassantin analogues (**MA04**, **MA07**, and **MA11**) based on their potency (from luciferase-reporter assay), lack of general toxicity (from MTT assay), and structural simplicity. After incubating HEK-293T cells under hypoxia (1% O₂) for 24 h with or without compounds, total protein lysate was extracted. Western blots were performed following the standard procedures. Compounds **MA04**, **MA07**, and **MA11** at 1 μM significantly down-regulated the expression level of HIF-1α in HEK-293T cells under hypoxia (Figure 3A). To determine whether **MA04**, **MA07**, or **MA11** regulates HIF-1β, a transcription partner of HIF-1α, we performed Western blot analysis with antibody against HIF-1β. Compounds **MA04**, **MA07**, and **MA11** did not regulate HIF-1β as in the case of **1**, suggesting that **MA04**, **MA07**, and **MA11** regulate HIF-1α but not HIF-1β.

To further confirm the effects of **MA04**, **MA07**, and **MA11** on HIF-1 activity, we determined the effect on HIF target genes at the transcriptional level. Upon treatment of **MA04**, **MA07**, or **MA11** at 1 μM, the protein level of cyclin-dependent kinase 6 (Cdk6), which is a HIF-1 target gene that regulates cell cycle progression, was decreased under hypoxic conditions (Figure 3A). VEGF (a key angiogenic factor and a main target for HIF-1) mRNA levels were significantly reduced by **MA04** and to a lesser extent by **MA07** or **MA11** (Figure 3B). All together, these data demonstrate that **MA04**, **MA07**, and **MA11** are inhibitors of HIF-1 activity. These compounds may serve as

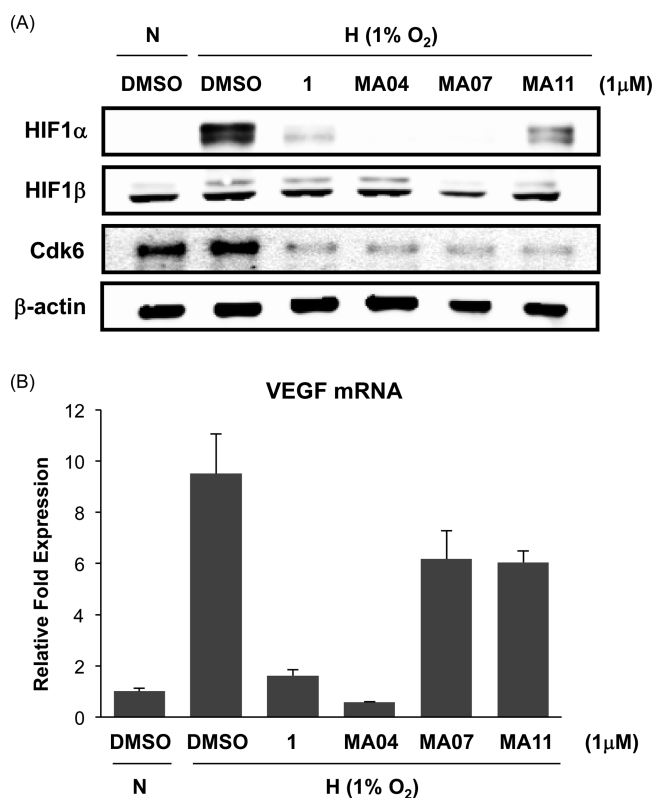


Figure 3. Manassantin A (**1**), MA04, MA07, and MA11 inhibit the expression of hypoxia-induced HIF-1α and HIF-1 target genes. (A) HEK-293T cells were treated with 1 μM of **1**, MA04, MA07, or MA11 under hypoxia for 24 h. HIF-1α, HIF-1β, and Cdk6 expression levels were determined by Western blot analysis with β-actin as an internal control (N, normoxia; H, hypoxia). (B) Relative expression of VEGF mRNA was determined by real-time PCR after treatment of cells with 1 μM of **1**, MA04, MA07, or MA11 under hypoxic conditions for 24 h. Relative expression of VEGF was normalized against β-actin (N, normoxia; H, hypoxia).

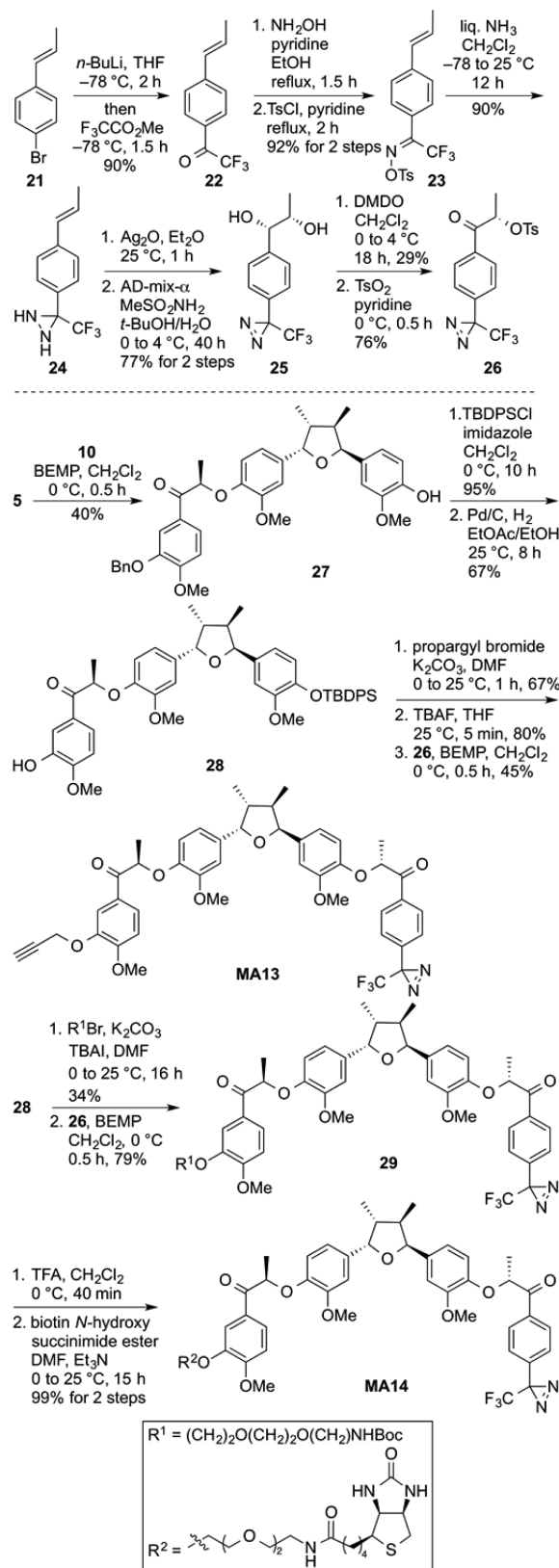
potential lead compounds for future *in vivo* animal and preclinical studies for novel anticancer drug development.

Photo-Cross-Linking Probes. Among various methods for molecular target identification,⁴⁰ small molecule affinity chromatography exploits the ability of small molecule probes to specifically bind to their molecular targets.⁴¹ This approach has led to the discovery of important drug targets such as histone deacetylases⁴² and splicing factor SF3b.⁴³ In particular, the approach can be very effective when a probe possesses an electrophile or a photo-cross-linking group to form a covalent linkage to its target proteins. Due to our strong interest in establishing the modes of action of manassantins, we designed and synthesized photo-cross-linking probes for future molecular target identification studies.

Among the commonly used photophores, the (3-trifluoromethyl)phenyldiazirine group is most popular owing to its wavelength for activation, the size of the photophore, cross-linking yields, side reactions, and stability of labeled products.⁴⁴ The carbene species generated from the diazirine group are strongly electrophilic and immediately insert into the target protein. On the basis of the SAR analysis described above, we designed two complementary photo-cross-linking probes (MA13 and MA14) by incorporation of a (3-trifluoromethyl)phenyldiazirine group as the cross-linking group and an alkyne or a biotin as the handle for protein

isolation (Scheme 6). These photo-cross-linking probes (MA13 and MA14) were easily prepared as illustrated in Scheme 6. After the preparation of MA13 and MA14, we evaluated the

Scheme 6. Synthesis of Photo-cross-linking Probes (MA13 and MA14)



activity of MA13 and MA14 in the dual luciferase-reporter assay as described above. MA13 and MA14 showed IC₅₀ values of 0.73 μM and 2.32 μM (see the Supporting Information for details), respectively, which was in accordance with our SAR analysis. After further biological evaluations of MA13, we plan to use MA13 in a small molecule affinity pull-down experiment side-by-side with other target identification approaches such as global gene expression^{45,46} and energetics-based proteomics.^{47,48}

CONCLUSION

Under hypoxia, tumors increase angiogenesis and metastatic potential, alter apoptosis, and regulate metabolism to cope with the stress of hypoxia. These adaptations make tumors more aggressive and treatment-resistant resulting in poor patient prognosis. HIF-1 is a main regulator of these adaptations through the activation of several hundred genes involved in angiogenesis, glucose transport, glycolytic pathway, ROS signals, erythropoiesis, and other processes. Due to the importance of HIF-1 in tumor development and progression, we have been exploring manassantins A (1) and B (2), potent inhibitors of HIF-1 activity isolated from *Saururus cernuus*, as effective therapeutics for cancers.

We prepared and evaluated a series of manassantin analogues for HIF-1α inhibition. The SAR study of manassantin analogues provided valuable insights into the role/function of the side chains of manassantins and their effects on hypoxia signaling. Among the analogues tested, MA04, MA07, and MA11 with reduced structural complexity down-regulated hypoxia-induced HIF-1α protein stabilization and reduced the levels of Cdk6 and VEGF under hypoxia. Moreover, two photo-cross-linking probes (MA13 and MA14) for molecular target identification were designed and synthesized on the basis of our SAR analysis. We expect that our findings will be an important basis for the future design of new manassantin analogues and optimization of drug-like properties of analogues for novel therapeutic development for cancers.

EXPERIMENTAL SECTION

General Procedures. All reactions were conducted in oven-dried glassware under nitrogen. Unless otherwise stated all reagents were purchased from Sigma–Aldrich, Acros, or Fisher and were used without further purification. All solvents were ACS grade or better and used without further purification except tetrahydrofuran (THF), which was freshly distilled from sodium/benzophenone each time before use. Analytical thin layer chromatography (TLC) was performed with glass backed silica gel (60 Å) plates with fluorescent indication (Whatman). Visualization was accomplished by UV irradiation at 254 nm or by staining with *p*-anisaldehyde solution. Flash column chromatography was performed by using silica gel (particle size 230–400 mesh, 60 Å). All ¹H NMR and ¹³C NMR spectra were recorded with a Varian 400 (400 MHz) and a Bruker 500 (500 MHz) spectrometer in CDCl₃ by using the signal of residual CHCl₃ as an internal standard. All NMR δ values are given in ppm, and all *J* values are in Hz. Electrospray ionization (ESI) mass spectrometry (MS) was recorded with an Agilent 1100 series (LC/MSD trap) spectrometer and performed to obtain the molecular masses of the compounds. Infrared (IR) absorption spectra were determined with a Thermo-Fisher (Nicolet 6700) spectrometer. Optical rotation values were measured with a Rudolph Research Analytical (A21102 API/1W) polarimeter. The percentage purity of compounds was above 95% as determined by HPLC.

(*E*)-2-(Benzyloxy)-1-methoxy-4-(prop-1-en-1-yl)benzene (7). To a cooled (0 °C) solution of the known *trans-m*-propenyl guaiacol (6;³¹ 867 mg, 5.28 mmol) in dry DMF (13 mL, 0.4 M) were added NaH

(60% dispersion in mineral oil, 304 mg, 7.92 mmol) and BnBr (0.63 mL, 5.28 mmol). The reaction mixture was allowed to warm to 25 °C. After stirring for 15 min, the reaction was quenched by addition of H₂O and extracted with EtOAc. The combined organic layers were washed with brine, dried over anhydrous Na₂SO₄, and concentrated *in vacuo*. The residue was purified by column chromatography (silica gel, hexanes/EtOAc, 20/1) to afford 7 as a white powder (1.22 g, 91%): ¹H NMR (400 MHz, CDCl₃) δ 7.50 (d, *J* = 8.0 Hz, 2H), 7.41 (t, *J* = 8.0 Hz, 2H), 7.35 (d, *J* = 7.2 Hz, 1H), 6.98 (s, 1H), 6.92 (d, *J* = 7.2 Hz, 1H), 6.85 (d, *J* = 8.4 Hz, 1H), 6.34 (d, *J* = 15.6 Hz, 1H), 6.07 (dq, *J* = 6.8, 15.6 Hz, 1H), 5.19 (s, 2H), 3.89 (s, 3H), 1.89 (d, *J* = 6.8 Hz, 3H); ¹³C NMR (125 MHz, CDCl₃) δ 148.9, 148.2, 137.2, 131.1, 130.6, 128.5, 127.4, 127.3, 123.6, 119.2, 111.8, 111.5, 71.0, 55.9, 18.3; IR (neat) 2932, 1510, 1258, 1136, 1024, 962 cm⁻¹; HRMS (ESI) *m/z* 255.1389 [(M + H)⁺, C₁₇H₁₈O₂ requires 255.1380].

(1*S*,2*S*)-1-(3-(Benzyloxy)-4-methoxyphenyl)propane-1,2-diol (8). To a cooled (0 °C) solution of AD-mix-α (5.06 g, 1.4 g/gmmol of substrate) and MeSO₂NH₂ (344 mg, 3.62 mmol) in *t*-BuOH/H₂O (1/2, 31.5 mL) was added dropwise alkene 7 (920 mg, 3.62 mmol) in EtOAc/*t*-BuOH (1/2, 16 mL). The reaction mixture was stirred for 2 days at 4 °C. The reaction was quenched by addition of sodium sulfite (5.42 g, 1.5 g/gmmol of substrate), diluted with EtOAc, and stirred for 30 min at 25 °C. The layers were separated, and the aqueous layer was extracted with EtOAc. The combined organic layers were washed with 2 N KOH and brine, dried over anhydrous Na₂SO₄, and concentrated *in vacuo*. The residue was purified by column chromatography (silica gel, hexanes/EtOAc, 1/1) to afford 8 as a colorless oil (834 mg, 80%): ¹H NMR (400 MHz, CDCl₃) δ 7.42 (d, *J* = 7.2 Hz, 2H), 7.35 (t, *J* = 7.2 Hz, 2H), 7.29 (d, *J* = 7.2 Hz), 6.87–6.85 (m, 3H) 4.21 (d, *J* = 7.6 Hz, 1H), 3.86 (s, 1H), 3.72 (dq, *J* = 6.4, 14.0 Hz, 1H), 2.71 (br s, 2H), 0.94 (d, *J* = 6.4 Hz, 3H); ¹³C NMR (125 MHz, CDCl₃) δ 149.4, 147.9, 136.9, 133.7, 128.4, 127.8, 127.5, 119.9, 113.0, 111.6, 79.1, 72.1, 71.0, 55.9, 18.7; IR (neat) 3383, 2970, 1733, 1513, 1256, 1134, 1021 cm⁻¹; HRMS (ESI) *m/z* 311.1244 [(M + Na)⁺, C₁₇H₂₀O₄ requires 311.1254].

(*S*)-1-(3-(Benzyloxy)-4-methoxyphenyl)-2-hydroxypropan-1-one (9). To a solution of diol 8 (834 mg, 2.89 mmol) in dioxane (29 mL, 0.1 M) was added DDQ (1.31 g, 5.78 mmol) at 25 °C. The reaction mixture was heated to 60 °C and stirred for 2 h at the same temperature. The reaction mixture was cooled to 0 °C, quenched by addition of saturated aqueous sodium thiosulfate and saturated aqueous NaHCO₃, diluted with CH₂Cl₂, and stirred vigorously for 1 h. The layers were separated, and the aqueous layer was extracted with CH₂Cl₂. The combined organic layers were washed with brine, dried over anhydrous Na₂SO₄, and concentrated *in vacuo*. The residue was purified by column chromatography (silica gel, hexanes/EtOAc, 2/1) to afford 9 as a yellow oil (762 mg, 92%): ¹H NMR (400 MHz, CDCl₃) δ 7.56–7.52 (m, 2H), 7.47–7.45 (m, 2H), 7.39 (dd, *J* = 7.2, 8.0 Hz, 2H), 7.33 (d, *J* = 7.6 Hz, 1H), 6.93 (d, *J* = 8.4 Hz, 1H), 5.20 (s, 2H), 5.04 (q, *J* = 7.2 Hz, 1H), 3.96 (s, 3H), 1.37 (d, *J* = 7.2 Hz); ¹³C NMR (125 MHz, CDCl₃) δ 200.7, 154.2, 148.3, 136.5, 128.7, 128.2, 127.5, 126.1, 123.8, 113.5, 110.8, 71.1, 68.9; IR (neat) 3459, 2976, 1667, 1594, 1512, 1263, 1114, 1016, 861 cm⁻¹; HRMS (ESI) *m/z* 287.1269 [(M + H)⁺, C₁₇H₁₈O₄ requires 287.1278].

(*S*)-1-(3-(Benzyloxy)-4-methoxyphenyl)-1-oxopropan-2-yl-4-methylbenzenesulfonate (10). To a cooled (0 °C) solution of hydroxyketone 9 (750 mg, 2.62 mmol) in pyridine (25 mL, 0.1 M) was added Ts₂O (1.28 g, 3.93 mmol). After stirring for 40 min at the same temperature, the reaction was quenched by addition of saturated aqueous NH₄Cl and extracted with CH₂Cl₂. The combined organic layers were washed with brine, dried over anhydrous Na₂SO₄, and concentrated *in vacuo*. The residue was purified by column chromatography (silica gel, hexanes/EtOAc, 2/1) to afford 10 as a white powder (935 mg, 81%): ¹H NMR (400 MHz, CDCl₃) δ 7.71 (d, *J* = 8.4 Hz, 2H), 7.54 (dd, *J* = 2.0, 8.8 Hz, 1H), 7.46–7.41 (m, 3H), 7.36–7.32 (m, 2H), 7.30–7.28 (m, 1H), 7.22 (d, *J* = 8.4 Hz, 2H), 6.86 (d, *J* = 8.8 Hz, 1H), 5.69 (q, *J* = 7.2 Hz, 1H), 5.12 (s, 2H), 3.90 (s, 3H), 2.36 (s, 3H), 1.48 (d, *J* = 7.2 Hz, 3H); ¹³C NMR (125 MHz, CDCl₃) δ 192.9, 154.7, 148.3, 145.0, 136.5, 133.6, 129.8, 128.6, 128.1, 127.9, 127.6, 126.5, 123.9, 113.4, 110.7, 77.2, 71.0, 56.2, 21.6, 18.9; IR

(neat) 2961, 1684, 1594, 1515, 1265, 1175, 1013, 932 cm^{-1} ; HRMS (ESI) m/z 441.1356 [(M + H)⁺, C₂₄H₂₄O₆S requires 441.1366].

(2*R*,2'*R*)-2,2'-(((2*S*,3*R*,4*R*,5*S*)-3,4-Dimethyltetrahydrofuran-2,5-diyloxy)bis(2-methoxy-4-1-phenylene))bis(oxy)bis(1-[3-(benzyloxy)-4-methoxyphenyl]propan-1-one) (**13**). To a cooled (0 °C) solution of the known bis-phenol tetrahydrofuran core **5**²⁴ (54 mg, 0.16 mmol) in dry CH₂Cl₂ (2 mL, 0.08 M) was added dropwise 2-*tert*-butylimino-2-diethylamino-1,3-dimethylperhydro-1,3,2-diazaphosphorine (BEMP, 0.09 mL, 0.31 mmol). The resulting mixture was stirred at the same temperature for 10 min before tosylate **10** (207.2 mg, 0.47 mmol) in CH₂Cl₂ (2 mL, 0.23 M) was added. After stirring for 30 min at 0 °C, the reaction was quenched by addition of saturated aqueous NH₄Cl and extracted with CH₂Cl₂. The combined organic layers were washed with brine, dried over anhydrous Na₂SO₄, and concentrated *in vacuo*. The residue was purified by column chromatography (silica gel, hexanes/EtOAc, 2/1) to afford **13** as a white foam (133 mg, 96%): ¹H NMR (400 MHz, CDCl₃) δ 7.82–7.76 (m, 4H), 7.46 (d, J = 7.6 Hz, 4H), 7.36 (dd, J = 7.2, 8.0 Hz, 4H), 7.31 (dd, J = 2.4, 7.2 Hz, 2H), 6.89 (d, J = 8.4 Hz, 2H), 6.82 (dd, J = 2.0, 10.0 Hz, 2H), 6.76–6.73 (m, 2H), 6.69 (dd, J = 1.6, 8.4 Hz, 2H), 5.36–5.32 (m, 4H), 5.17 (s, 4H), 3.92 (s, 6H), 3.83 (s, 6H), 2.23–2.17 (m, 2H), 1.64 (d, J = 6.8 Hz, 6H), 0.62 (d, J = 6.4 Hz, 6H); ¹³C NMR (125 MHz, CDCl₃) δ 197.5, 154.2, 150.0, 147.9, 145.8, 136.6, 135.6, 128.6, 128.0, 127.6, 127.3, 123.9, 118.5, 115.7, 113.9, 110.6, 110.5, 83.4, 78.3, 70.8, 56.0, 44.0, 19.1, 14.8; IR (neat) 2961, 1684, 1593, 1509, 1265, 1137, 1020, 867 cm^{-1} ; HRMS (ESI) m/z 898.4169 [(M + NH₄)⁺, C₅₄H₅₆O₁₁ requires 898.4161].

MA01. To a stirred solution of bis-benzyl ether **13** (29 mg, 0.03 mmol) in EtOAc (2 mL, 0.02M) was added 10% Pd–C (6 mg, 20 wt %) The resulting mixture was stirred under H₂ atmosphere at 25 °C for 8 h. The reaction mixture was then filtered through Celite with EtOAc and concentrated *in vacuo*. The residue was purified by column chromatography (silica gel, hexanes/EtOAc, 3/2) to afford **MA01** as a white foam (22.1 mg, 96%): [α]_D²⁵ = –19.9 (c 0.73, CHCl₃); ¹H NMR (400 MHz, CDCl₃) δ 7.73–7.68 (m, 4H), 6.87 (dd, J = 1.6, 8.4 Hz, 2H), 6.80 (dd, J = 1.6, 6.0 Hz, 2H), 6.77–6.73 (m, 2H), 6.67 (dd, J = 1.6, 8.4 Hz, 2H), 5.71 (br s, 2H), 5.40 (ddd, J = 6.8, 6.8, 6.8 Hz, 2H), 5.34 (d, J = 6.0 Hz), 3.93 (s, 6H), 3.83 (s, 6H), 2.20–2.16 (m, 2H), 1.67 (dd, J = 2.4, 6.8 Hz, 6H), 0.61 (d, J = 6.4 Hz, 6H); ¹³C NMR (125 MHz, CDCl₃) δ 197.8, 151.1, 150.0, 146.0, 145.6, 135.8, 128.3, 122.7, 118.6, 116.4, 116.1, 115.2, 110.8, 110.1, 83.6, 78.2, 56.2, 44.1, 19.2, 14.8; IR (neat) 3404, 2962, 1684, 1608, 1509, 1272, 1139, 1028, 866 cm^{-1} ; HRMS (ESI) m/z 701.2951 [(M + H)⁺, C₄₀H₄₄O₁₁ requires 701.2956].

MA02. To a cooled (0 °C) solution of bis-phenol **MA01** (44 mg, 0.06 mmol) in dry CH₂Cl₂ (1.5 mL, 0.04 M) was added dropwise BEMP (0.04 mL, 0.13 mmol). The resulting mixture was stirred at the same temperature for 10 min before the known bromide **12**³³ (65 mg, 0.25 mmol) in CH₂Cl₂ (1.5 mL, 0.17 M) was added. After stirring for 1 h at 0 °C, the reaction was quenched by addition of saturated aqueous NH₄Cl and extracted with CH₂Cl₂. The combined organic layers were washed with brine, dried over anhydrous Na₂SO₄, and concentrated *in vacuo*. The residue was purified by column chromatography (silica gel, hexanes/EtOAc, 1/2) to afford **MA02** as a yellow foam (52.6 mg, 80%): [α]_D^{22.6} = 7.9 (c 0.66, CHCl₃); ¹H NMR (400 MHz, CDCl₃) δ 7.86–7.82 (m, 2H), 7.61 (dd, J = 2.0, 6.4 Hz, 4H), 7.54 (s, 2H), 6.90 (dd, J = 6.0, 8.8 Hz, 4H), 6.79 (dd, J = 1.6, 8.8 Hz, 2H), 6.73 (dd, J = 4.8, 8.4 Hz, 2H), 6.68–6.64 (m, 2H), 5.40–5.31 (m, 8H), 3.95–3.92 (m, 18H), 3.80 (s, 6H), 2.19–2.15 (m, 2H), 1.65 (d, J = 6.8 Hz, 6H), 0.60 (d, J = 6.4 Hz, 6H); ¹³C NMR (125 MHz, CDCl₃) δ 197.4, 192.2, 154.2, 154.0, 149.8, 149.4, 147.5, 145.8, 135.7, 127.8, 127.4, 124.7, 122.7, 118.5, 116.0, 113.8, 110.9, 110.7, 110.4, 110.3, 83.4, 78.3, 71.1, 56.2, 44.0, 19.1, 14.8; IR (neat) 2932, 1685, 1595, 1513, 1266, 1134, 1021, 870 cm^{-1} ; HRMS (ESI) m/z 1074.4497 [(M + NH₄)⁺, C₆₀H₆₄O₁₇ requires 1074.4482].

MA03. To a solution of the known phenol **15**²⁴ (32 mg, 0.06 mmol) in acetone (3 mL, 0.02 M) was added K₂CO₃ (16.6 mg, 0.12 mmol) at 25 °C. After stirring for 1 h at 40 °C, the reaction mixture was cooled to 25 °C and treated with MeI (0.02 mL, 0.24 mmol) at the same temperature. After stirring for 2 h at reflux, the reaction

mixture was cooled to 25 °C, diluted with EtOAc, and rinsed with saturated aqueous NH₄Cl. The layers were separated, and the aqueous layer was extracted with EtOAc. The combined organic layers were washed with brine, dried over anhydrous Na₂SO₄, and concentrated *in vacuo*. The residue was purified by column chromatography (silica gel, hexanes/EtOAc, 1/1) to afford **MA03** as a white foam (31 mg, 93%): [α]_D^{22.4} = –22.5 (c 0.13, EtOAc); ¹H NMR (400 MHz, CDCl₃) δ 7.84–7.80 (m, 1H), 7.68–7.66 (m, 1H), 6.87–6.67 (m, 7H), 5.44–5.36 (m, 3H), 3.93 (s, 3H), 3.91 (s, 3H), 3.87 (s, 3H), 3.86 (s, 3H), 3.85 (s, 3H), 2.25–2.19 (m, 2H), 1.71 (d, J = 6.8 Hz, 3H), 0.65 (dd, J = 6.4, 7.2 Hz, 3H); ¹³C NMR (125 MHz, CDCl₃) δ 197.9, 153.7, 149.8, 149.1, 148.7, 148.0, 146.4, 145.9, 135.8, 134.0, 127.6, 123.7, 118.6, 115.9, 111.4, 110.9, 110.7, 110.2, 109.7, 109.0, 83.6, 78.5, 56.1, 44.2, 19.3, 14.9; IR (neat) 2960, 1682, 1593, 1512, 1261, 1136, 1023, 799 cm^{-1} ; HRMS (ESI) m/z 551.2631 [(M + H)⁺, C₃₂H₃₈O₈ requires 551.2639].

MA04. To a stirred solution of **MA03** (31 mg, 0.06 mmol) in MeOH (2 mL, 0.02 M) was added polymer-supported borohydride (2 mmol BH₄/g resin, 560 mg, 1.12 mmol). The reaction mixture was stirred with gentle agitation at 25 °C for 72 h. The polymer beads were then removed by filtration, and the filtrate was purified by column chromatography (silica gel, hexanes/EtOAc, 4/1) to afford **MA04** as a colorless oil (25 mg, 80%): [α]_D^{22.5} = –78.3 (c 0.52, CHCl₃); ¹H NMR (400 MHz, CDCl₃) δ 7.00–6.82 (m, 9H), 5.45 (d, J = 6.0 Hz, 2H), 4.64 (d, J = 8.4 Hz, 1H), 4.15–4.08 (m, 1H), 3.92 (s, 3H), 3.89 (s, 3H), 3.88 (s, 6H), 3.87 (s, 3H), 2.22–2.31 (m, 2H), 1.17 (d, J = 6.4 Hz, 3H), 0.71 (d, J = 6.4 Hz, 3H), 0.69 (dd, J = 6.4, 6.4 Hz, 3H); ¹³C NMR (125 MHz, CDCl₃) δ 150.7, 149.1, 149.0, 148.8, 148.0, 146.6, 136.8, 134.0, 132.7, 120.1, 118.8, 118.5, 111.0, 110.9, 110.3, 110.2, 109.7, 84.3, 83.6, 83.5, 78.5, 56.0, 44.2, 17.2, 14.9; IR (neat) 3453, 2930, 1510, 1256, 1138, 1027, 811, 733 cm^{-1} ; HRMS (ESI) m/z 570.3072 [(M + NH₄)⁺, C₃₂H₄₀O₈ requires 570.3061].

MA06. To a cooled (0 °C) solution of manassantin A (25 mg, 0.03 mmol) in THF (2 mL, 0.02 M) were added NaH (60% dispersion in mineral oil, 10.5 mg, 0.27 mmol) and MeI (0.02 mL, 0.34 mmol). After stirring for 1 h at the same temperature, the reaction was quenched by addition of H₂O and extracted with EtOAc. The combined organic layers were washed with brine, dried over anhydrous Na₂SO₄, and concentrated *in vacuo*. The residue was purified by column chromatography (silica gel, hexanes/EtOAc, 2/1) to afford **MA06** as a colorless oil (23 mg, 79%): [α]_D^{23.2} = –49.9 (c 0.3, CHCl₃); ¹H NMR (400 MHz, CDCl₃) δ 6.97–6.77 (m, 12H), 5.42 (d, J = 6.4 Hz, 2H), 4.53–4.46 (m, 2H), 4.32 (d, J = 6.4 Hz, 2H), 3.90 (s, 6H), 3.89 (s, 6H), 3.85 (s, 6H), 3.29 (s, 6H), 2.28–2.22 (m, 2H), 1.06 (d, J = 6.4 Hz, 6H), 0.68 (d, J = 6.4 Hz, 6H); ¹³C NMR (125 MHz, CDCl₃) δ 150.5, 149.2, 148.9, 146.8, 135.1, 131.4, 120.5, 118.7, 116.6, 110.8, 110.6, 86.6, 83.7, 79.0, 57.3, 56.2, 56.1, 44.2, 16.5, 15.0; IR (neat) 2933, 1508, 1271, 1028 cm^{-1} ; HRMS (ESI) m/z 778.4153 [(M + NH₄)⁺, C₄₄H₅₆O₁₁ requires 778.4161].

MA07. To a cooled (0 °C) solution of the known bis-phenol **5** (90 mg, 0.26 mmol) in dry DMF (2 mL, 0.13 M) was added NaH (60% dispersion in mineral oil, 30 mg, 0.78 mmol). After stirring for 5 min, the reaction mixture was treated with the known bromide **12**³³ (271 mg, 1.04 mmol) in DMF (4 mL, 0.26 M) and stirred for 40 min. The resulting mixture was allowed to warm to 25 °C for 2 h. At 0 °C, the reaction was quenched by addition of saturated aqueous NH₄Cl and extracted with EtOAc. The combined organic layers were washed with brine, dried over anhydrous Na₂SO₄, and concentrated *in vacuo*. The residue was purified by column chromatography (silica gel, hexanes/EtOAc, 1/1) to afford **MA07** as a colorless oil (90 mg, 47%): [α]_D^{25.0} = –25.7 (c 0.4, EtOAc); ¹H NMR (400 MHz, CDCl₃) δ 7.67 (dd, J = 2.0, 8.4 Hz, 2H), 7.59 (s, 2H), 6.90–6.73 (m, 8H), 5.40 (d, J = 6.0 Hz, 2H), 5.28 (s, 4H), 3.95 (s, 6H), 3.93 (s, 6H), 3.89 (s, 6H), 2.26–2.20 (m, 2H), 0.66 (d, J = 6.4 Hz, 6H); ¹³C NMR (125 MHz, CDCl₃) δ 193.5, 153.9, 149.5, 149.3, 146.6, 135.7, 128.0, 122.9, 118.5, 114.5, 110.6, 110.4, 110.2, 83.5, 72.4, 56.2, 56.1, 44.2, 14.9; IR (neat) 2931, 1689, 1512, 1261, 1163, 1021 cm^{-1} ; HRMS (ESI) m/z 701.2959 [(M + H)⁺, C₄₀H₄₄O₁₁ requires 701.2956].

MA08. To a cooled (–20 °C) solution of (*R*)-(+)-2-methyl-CBS-oxazaborolidine (0.69 mg, 2.5 μmol) and BH₃·SMe₂ (5 μL , 0.05

mmol) in toluene (1 mL, 0.05 M) was added dropwise ketone **MA07** (35 mg, 0.05 mmol) in toluene (2 mL, 0.03 M). After stirring for 1 h at the same temperature, the reaction was quenched by addition of MeOH followed by 1 N HCl. The aqueous layer was extracted with EtOAc, dried over anhydrous Na₂SO₄, and concentrated *in vacuo*. The residue was purified by column chromatography (silica gel, hexanes/EtOAc, 1/2) to afford **MA08** as a colorless oil (29 mg, 82%): $[\alpha]_D^{20} = -32.9$ (c 0.4, EtOAc); ¹H NMR (400 MHz, CDCl₃) δ 7.01–6.80 (m, 12H), 5.44 (d, *J* = 6.0 Hz, 2H), 5.05 (dd, *J* = 2.8, 9.2 Hz, 2H), 4.15 (dd, *J* = 3.2, 10.4 Hz, 2H), 3.96 (t, *J* = 10.0 Hz, 2H), 3.894 (s, 6H), 3.89 (s, 6H), 3.87 (s, 6H), 3.30 (br s, 2H), 2.31–2.23 (m, 2H), 0.69 (d, *J* = 6.4 Hz, 6H); ¹³C NMR (125 MHz, EtOAc) δ 149.9, 149.2, 148.9, 146.9, 135.8, 132.3, 118.8, 118.7, 115.6, 111.1, 110.2, 109.5, 83.5, 76.5, 72.2, 56.0, 44.2, 14.9; IR (neat) 3481, 2922, 1514, 1262, 1027, 810 cm⁻¹; HRMS (ESI) *m/z* 722.3523 [(M + NH₄)⁺, C₄₀H₄₈O₁₁ requires 722.3535].

MA09. To a cooled (0 °C) solution of alcohol **MA08** (24 mg, 0.03 mmol) in dry DMF (3 mL, 0.01 M) were added NaH (60% dispersion in mineral oil, 20.5 mg, 0.55 mmol) and MeI (0.04 mL, 0.68 mmol). After stirring for 1 h at the same temperature, the reaction was quenched by addition of H₂O and extracted with EtOAc. The combined organic layers were washed with brine, dried over anhydrous Na₂SO₄, and concentrated *in vacuo*. The residue was purified by column chromatography (silica gel, hexanes/EtOAc, 2/3) to afford **MA09** as a white foam (23 mg, 92%): $[\alpha]_D^{22.0} = -43.2$ (c 0.38, EtOAc); ¹H NMR (400 MHz, CDCl₃) δ 6.95–6.75 (m, 12H), 5.41 (d, *J* = 5.6 Hz, 2H), 4.60 (dd, *J* = 3.2, 7.6 Hz, 2H), 4.18 (dd, *J* = 8.0, 10.8 Hz, 2H), 4.02 (dd, *J* = 3.6, 6.8 Hz, 2H), 3.90 (s, 6H), 3.88 (s, 6H), 3.86 (s, 6H), 3.35 (s, 6H), 2.26–2.20 (m, 2H), 0.66 (d, *J* = 6.4 Hz, 6H); ¹³C NMR (125 MHz, CDCl₃) δ 149.6, 149.3, 149.0, 135.0, 131.4, 119.6, 118.5, 114.1, 111.1, 110.5, 109.9, 83.6, 82.2, 74.0, 57.2, 56.1, 56.0, 44.2, 14.9; IR (neat) 2932, 1513, 1261, 1137, 1028 cm⁻¹; HRMS (ESI) *m/z* 750.3846 [(M + NH₄)⁺, C₄₂H₅₂O₁₁ requires 750.3848].

MA10. To a solution of the known bis-phenol **5** (20 mg, 0.06 mmol) in dry DMF (1.5 mL, 0.04 M) were added K₂CO₃ (32 mg, 0.23 mmol) and 3,4-dimethoxyphenethyl bromide (143 mg, 0.58 mmol) at 25 °C. The reaction mixture was heated to 120 °C and stirred for 30 h at the same temperature. The reaction was quenched by addition of saturated aqueous NH₄Cl and extracted with EtOAc. The combined organic layers were washed with brine, dried over anhydrous Na₂SO₄, and concentrated *in vacuo*. The residue was purified by column chromatography (silica gel, hexanes/EtOAc, 3/1) to afford **MA10** as a yellow oil (18 mg, 44%): $[\alpha]_D^{21.8} = -6.79$ (c 0.28, EtOAc); ¹H NMR (400 MHz, CDCl₃) δ 6.87–6.82 (m, 12H), 5.43 (d, *J* = 6.0 Hz, 2H), 4.19 (t, *J* = 7.2 Hz, 4H), 3.88–3.87 (m, 18H), 3.10 (t, *J* = 7.2 Hz, 4H), 2.29–2.22 (m, 2H), 0.68 (d, *J* = 6.0 Hz, 6H); ¹³C NMR (125 MHz, CDCl₃) δ 149.2, 149.0, 147.8, 147.3, 134.5, 130.9, 121.1, 118.6, 112.9, 112.6, 111.4, 110.3, 83.6, 70.2, 56.2, 56.1, 55.9, 56.2, 56.1, 55.9, 44.2, 35.6, 14.9; IR (neat) 2928, 1507, 1229, 1138, 1026 cm⁻¹; HRMS (ESI) *m/z* 690.3632 [(M + NH₄)⁺, C₄₀H₄₈O₉ requires 690.3637].

(1S,2S)-1-Phenylpropane-1,2-diol (18). To a cooled (0 °C) solution of AD-mix- α (5.4 g, 1.4 g/mmol of substrate) and MeSO₂NH₂ (367 mg, 3.85 mmol) in *t*-BuOH/H₂O (1/2, 30 mL) was added dropwise *trans*- β -methylstyrene **17** (0.5 mL, 3.85 mmol) in *t*-BuOH (10 mL). The reaction mixture was stirred for 48 h at 4 °C. The reaction was quenched by addition of sodium sulfite (5.78 g, 1.5 g/mmol of substrate), diluted with EtOAc, and stirred for 30 min at 25 °C. The layers were separated, and the aqueous layer was extracted with EtOAc. The combined organic layers were washed with 2 N KOH and brine, dried over anhydrous Na₂SO₄, and concentrated *in vacuo*. The residue was purified by column chromatography (silica gel, hexanes/EtOAc, 3/1) to afford **18** as a colorless oil (539 mg, 92%): ¹H NMR (400 MHz, CDCl₃) δ 7.33–7.23 (m, 5H), 4.25 (d, *J* = 7.6 Hz, 1H), 4.02 (br s, 2H), 3.77 (dq, *J* = 6.4, 13.6 Hz, 1H), 0.95 (d, *J* = 6.4 Hz, 3H); ¹³C NMR (125 MHz, CDCl₃) δ 141.2, 128.4, 128.0, 127.0, 79.5, 72.1; IR (neat) 3362, 2973, 1454, 1265, 1128, 1036, 870 cm⁻¹; HRMS (ESI) *m/z* 135.0804 [M + H–H₂O, C₉H₁₂O₂ requires 135.0804].

(S)-2-Hydroxy-1-phenylpropan-1-one (19). To a solution of diol **18** (539 mg, 3.54 mmol) in dioxane (35 mL, 0.1 M) was added DDQ (1.6 g, 7.08 mmol) at 25 °C. The reaction mixture was heated to 80 °C and stirred for 12 h at the same temperature. The reaction mixture was cooled to 0 °C, quenched by addition of saturated aqueous sodium thiosulfate and saturated aqueous NaHCO₃, diluted with CH₂Cl₂, and stirred vigorously for 1 h. The layers were separated, and the aqueous layer was extracted with CH₂Cl₂. The combined organic layers were washed with brine, dried over anhydrous Na₂SO₄, and concentrated *in vacuo*. The residue was purified by column chromatography (silica gel, hexanes/EtOAc, 2/1) to afford **19** as a colorless crystal (308 mg, 58%): ¹H NMR (400 MHz, CDCl₃) δ 7.92 (dd, *J* = 1.2, 8.4 Hz, 2H), 7.63–7.58 (m, 1H), 7.49 (dt, *J* = 1.6, 7.6, 14.0 Hz, 2H), 5.16 (q, *J* = 7.2 Hz, 1H), 3.73 (br s, 1H), 1.44 (d, *J* = 7.2 Hz, 3H); ¹³C NMR (125 MHz, CDCl₃) δ 202.6, 134.1, 133.5, 128.9, 69.5, 22.4; IR (neat) 3455, 2979, 1679, 1597, 1268, 1126, 1025, 968 cm⁻¹; HRMS (ESI) *m/z* 133.0647 [(M + H – H₂O)⁺, C₉H₁₀O₂ requires 133.0648].

(S)-1-Oxo-1-phenylpropan-2-yl 4-methylbenzenesulfonate (20). To a cooled (0 °C) solution of hydroxyketone **19** (308 mg, 2.05 mmol) in pyridine (20 mL, 0.1 M) was added Ts₂O (1 g, 3.08 mmol). After stirring for 30 min at the same temperature, the reaction was quenched by addition of saturated aqueous NH₄Cl and extracted with CH₂Cl₂. The combined organic layers were washed with brine, dried over anhydrous Na₂SO₄, and concentrated *in vacuo*. The residue was purified by column chromatography (silica gel, hexanes/EtOAc, 2/1) to afford **20** as a white powder (437 mg, 70%): ¹H NMR (400 MHz, CDCl₃) δ 7.87 (dd, *J* = 1.2, 8.4 Hz, 2H), 7.75 (dd, *J* = 1.2, 8.4 Hz, 2H), 7.61–7.56 (m, 1H), 7.45 (dt, *J* = 1.6, 8.0, 13.6 Hz, 2H), 7.26 (d, *J* = 8.0 Hz, 2H), 5.78 (q, *J* = 7.2 Hz, 1H), 2.40 (s, 3H), 1.59 (d, *J* = 7.2 Hz, 3H); ¹³C NMR (125 MHz, CDCl₃) δ 194.9, 145.2, 134.0, 133.8, 133.6, 129.9, 128.9, 128.0, 77.5, 21.7, 18.8; IR (neat) 2960, 1699, 1597, 1360, 1175, 1017, 919 cm⁻¹; HRMS (ESI) *m/z* 305.0836 [(M + H)⁺, C₁₆H₁₆O₄S requires 305.0842].

MA11. To a cooled (0 °C) solution of the known bis-phenol **5** (30 mg, 0.09 mmol) in dry CH₂Cl₂ (1.5 mL, 0.06 M) was added dropwise BEMP (0.05 mL, 0.17 mmol). The resulting mixture was stirred at the same temperature for 10 min before tosylate **20** (106 mg, 0.35 mmol) in CH₂Cl₂ (1.5 mL, 0.23 M) was added. After stirring for 30 min at 0 °C, the reaction was quenched by addition of saturated aqueous NH₄Cl and extracted with CH₂Cl₂. The combined organic layers were washed with brine, dried over anhydrous Na₂SO₄, and concentrated *in vacuo*. The residue was purified by column chromatography (silica gel, hexanes/EtOAc, 4/1) to afford **MA11** as a colorless oil (45.5 mg, 86%): $[\alpha]_D^{23.4} = -27.57$ (c 0.5, CHCl₃); ¹H NMR (400 MHz, CDCl₃) δ 8.11–8.08 (m, 4H), 7.58–7.54 (m, 2H), 7.45 (dd, *J* = 6.0, 7.2 Hz, 4H), 6.82–6.77 (m, 4H), 6.70–6.66 (m, 2H), 5.46 (dq, *J* = 4.0, 6.8 Hz, 2H), 5.35 (d, *J* = 6.0 Hz, 2H), 3.82 (s, 6H), 2.22–2.16 (m, 2H), 1.70 (d, *J* = 7.2 Hz, 6H), 0.62 (d, *J* = 6.4 Hz, 6H); ¹³C NMR (125 MHz, CDCl₃) δ 199.3, 150.0, 145.9, 136.0, 134.8, 133.5, 129.1, 128.7, 118.6, 116.7, 116.5, 110.7, 83.5, 78.5, 56.1, 44.2, 30.0, 19.0, 14.9; IR (neat) 2962, 1697, 1508, 1269, 1221, 1142, 1034, 966 cm⁻¹; HRMS (ESI) *m/z* 626.3107 [(M + NH₄)⁺, C₃₈H₄₀O₇ requires 626.3112].

MA12. To a stirred solution of **11** (42 mg, 0.07 mmol) in MeOH (4.5 mL, 0.02 M) was added polymer-supported borohydride (2 mmol BH₄/g resin, 690 mg, 1.38 mmol). The reaction mixture was stirred with gentle agitation at 25 °C for 48 h. The polymer beads were then removed by filtration, and the filtrate was purified by column chromatography (silica gel, hexanes/EtOAc, 2/1) to afford **MA12** as a colorless oil (23 mg, 54%): $[\alpha]_D^{22.7} = -62.14$ (c 0.4, EtOAc); ¹H NMR (400 MHz, CDCl₃) δ 7.41–7.28 (m, 10H), 7.00–6.81 (m, 6H), 5.46 (d, *J* = 6.0 Hz, 2H), 4.70 (d, *J* = 8.0 Hz, 2H), 4.18–4.09 (m, 3H), 3.93 (s, 6H), 2.32–2.26 (m, 2H), 1.17 (dd, *J* = 2.0, 6.4 Hz, 6H), 0.72 (d, *J* = 6.4 Hz, 6H); ¹³C NMR (125 MHz, CDCl₃) δ 150.7, 146.6, 140.2, 136.7, 128.5, 128.2, 127.5, 119.0, 118.8, 110.3, 84.3, 83.5, 78.8, 56.0, 44.3, 17.1, 15.0; IR (neat) 3481, 2964, 1508, 1258, 1036 cm⁻¹; HRMS (ESI) *m/z* 630.3447 [(M + NH₄)⁺, C₃₈H₄₄O₇ requires 630.3425].

(E)-2,2,2-Trifluoro-1-[4-(prop-1-en-1-yl)phenyl]ethan-1-one (22). To a cooled (–78 °C) solution of (*E*)-1-bromo-4-(prop-1-en-1-yl)benzene⁴⁹ (340 mg, 1.73 mmol) in dry THF (15 mL, 0.12 M) was

added dropwise *n*-BuLi (2.3 M in hexane, 1.13 mL, 2.59 mmol). The resulting mixture was stirred for 2 h at the same temperature before methyl fluoroacetate (0.23 mL, 2.24 mmol) in dry THF (9 mL) was added dropwise. After stirring for 1.5 h at the same temperature, the reaction was quenched by addition of saturated aqueous NH₄Cl, and the resulting mixture was extracted with Et₂O. The combined organic layers were washed with brine, dried over anhydrous Na₂SO₄, and concentrated *in vacuo*. The residue was purified by column chromatography (silica gel, hexanes) to afford ketone **22** (337 mg, 90%): ¹H NMR (400 MHz, CDCl₃) δ 8.00 (d, *J* = 8.0 Hz, 2H), 7.46 (d, *J* = 8.4 Hz, 2H), 6.51–6.43 (m, 2H), 1.95 (d, *J* = 5.2 Hz, 3H).

(Z)-2,2,2-Trifluoro-1-[4-[(E)-prop-1-en-1-yl]phenyl]ethan-1-one Oxime Formation (23). Oxime Formation. To a solution of **22** (337 mg, 1.57 mmol) in pyridine/EtOH (2:1, 6 mL) was added hydroxylamine hydrochloride (142 mg, 2.05 mmol) at 25 °C. After stirring for 1.5 h at reflux, the solvents were removed under reduced pressure. The residue was extracted with EtOAc/H₂O, dried over anhydrous Na₂SO₄, and concentrated *in vacuo*. The crude residue was employed in the next step without further purification.

Tosylation. To a solution of the crude oxime (348 mg, 1.52 mmol) in pyridine (6 mL, 0.25 M) was added TsCl (434 mg, 2.28 mmol) at 25 °C. After stirring for 2 h at reflux, the solvents were removed under reduced pressure. The residue was extracted with EtOAc/H₂O, dried over anhydrous Na₂SO₄, and concentrated *in vacuo*. The residue was purified by column chromatography (silica gel, hexanes/EtOAc, 20/1) to afford tosyloxime **23** as a yellow powder (555 mg, 92% for 2 steps): ¹H NMR (400 MHz, CDCl₃) δ 7.91 (dd, *J* = 8.4, 14.4 Hz, 2H), 7.42–7.36 (m, 6H), 6.38 (dd, *J* = 4.0, 9.6 Hz, 2H), 2.48 (d, *J* = 5.6 Hz, 3H), 1.92 (d, *J* = 5.2 Hz, 3H).

(E)-3-[4-(Prop-1-en-1-yl)phenyl]-3-(trifluoromethyl)diaziridine (24). To a cooled (–78 °C) solution of **23** (550 mg, 1.43 mmol) in CH₂Cl₂ (10 mL, 0.14 M) was bubbled NH₃ gas. The resulting mixture was stirred in a sealed tube for 5 min at –78 °C and slowly warmed to 25 °C. After stirring for 12 h at the same temperature, the reaction mixture was cooled to –78 °C, and NH₃ was evaporated for 6 h at 25 °C. The solid was removed by filtration. The filtrate was washed with water and extracted with CH₂Cl₂. The combined organic layers were washed with brine, dried over anhydrous Na₂SO₄, and concentrated *in vacuo*. The residue was purified by column chromatography (silica gel, hexanes/EtOAc, 10/1) to afford diaziridine **24** (296 mg, 90%): ¹H NMR (400 MHz, CDCl₃) δ 7.53–7.49 (m, 2H), 7.37–7.32 (m, 2H), 6.43–6.36 (m, 1H), 6.30 (dq, *J* = 6.4, 19.2 Hz, 1H), 2.77 (br s, 1H), 2.20 (br s, 1H), 1.91–1.86 (m, 3H).

(1S,2S)-1-(4-[3-(Trifluoromethyl)-3H-diazirin-3-yl]phenyl)propane-1,2-diol (25). Oxidation. To a solution of **24** (290 mg, 1.27 mmol) in dry Et₂O (10 mL, 0.13 M) was added a freshly prepared Ag₂O (883 mg, 3.81 mmol) at 25 °C. After stirring for 1 h at the same temperature, the reaction mixture was filtered through Celite. The organic layers were dried over anhydrous Na₂SO₄ and concentrated *in vacuo*. The crude residue was employed in the next step without further purification.

Dihydroxylation. To a cooled (0 °C) solution of AD-mix-α (1.5 g, 1.4 g/mmol of substrate) and MeSO₂NH₂ (103 mg, 1.08 mmol) in *t*-BuOH/H₂O (1/2, 12 mL) was added dropwise the crude alkene (244 mg, 1.08 mmol) in *t*-BuOH (4 mL, 0.27 M). The reaction mixture was stirred for 40 h at 4 °C. The reaction was quenched by addition of sodium sulfite (1.55 g, 1.5 g/mmol of substrate). The resulting mixture was diluted with EtOAc and stirred for 30 min at 25 °C. The layers were separated, and the aqueous layer was extracted with EtOAc. The combined organic layers were washed with 2 N KOH and brine, dried over anhydrous Na₂SO₄, and concentrated *in vacuo*. The residue was purified by column chromatography (silica gel, hexanes/EtOAc, 3/2) to afford diol **25** (255 mg, 77% for 2 steps): ¹H NMR (400 MHz, CDCl₃) δ 7.38 (d, *J* = 8.4 Hz, 2H), 7.18 (d, *J* = 8.4 Hz, 2H), 4.40 (d, *J* = 7.2 Hz, 1H), 3.81 (m, 1H), 2.42 (br s, 2H), 1.07 (d, *J* = 6.4 Hz, 3H).

(S)-1-Oxo-1-(4-[3-(trifluoromethyl)-3H-diazirin-3-yl]phenyl)propan-2-yl 4-methylbenzenesulfonate (26). Oxidation. To a cooled (0 °C) solution of **25** (100 mg, 0.38 mmol) in CH₂Cl₂ (10 mL, 0.04 M) was added DMDO (0.1 M in acetone, 8.5 mL, 0.85 mmol). After stirring for 18 h at the same temperature, the solvents were removed

under reduced pressure. The residue was purified by column chromatography (silica gel, hexanes/EtOAc, 4/1) to afford the corresponding hydroxy ketone **S1** (29 mg, 29%): ¹H NMR (400 MHz, CDCl₃) δ 7.95 (d, *J* = 8.8 Hz, 2H), 7.31 (d, *J* = 8.0 Hz, 2H), 5.14 (dq, *J* = 6.4, 6.8 Hz, 1H), 3.65 (d, *J* = 6.8, 1H), 1.44 (d, *J* = 6.8 Hz, 3H).

Tosylation. To a cooled (0 °C) solution of **S1** (29 mg, 0.11 mmol) in pyridine (3 mL, 0.04 M) was added Ts₂O (55 mg, 0.17 mmol). After stirring for 30 min at the same temperature, the reaction was quenched by addition of saturated aqueous NH₄Cl and the resulting mixture was extracted with CH₂Cl₂. The combined organic layers were washed with brine, dried over anhydrous Na₂SO₄, and concentrated *in vacuo*. The residue was purified by column chromatography (silica gel, hexanes/EtOAc, 5/1) to afford tosylate **26** as a white powder (36 mg, 76%): ¹H NMR (400 MHz, CDCl₃) δ 7.91 (d, *J* = 8.8 Hz, 2H), 7.72 (d, *J* = 8.4 Hz, 2H), 7.26 (dd, *J* = 8.4, 8.4 Hz, 4H), 5.67 (q, *J* = 6.8 Hz, 1H), 2.42 (s, 3H), 1.58 (d, *J* = 6.8 Hz, 3H).

(R)-1-[3-(Benzyloxy)-4-methoxyphenyl]-2-(4-[(2S,3R,4R,5S)-5-(4-hydroxy-3-methoxyphenyl)-3,4-dimethyltetrahydrofuran-2-yl]-2-methoxyphenoxy)propan-1-one (27). To a cooled (0 °C) solution of the known bis-phenol **5** (35 mg, 0.1 mmol) in dry CH₂Cl₂ (1 mL, 0.1 M) was added dropwise BEMP (0.03 mL, 0.1 mmol). The resulting mixture was stirred at the same temperature for 10 min before tosylate **10** (45 mg, 0.1 mmol) in CH₂Cl₂ (1 mL, 0.1 M) was added. After stirring for 30 min at 0 °C, the reaction was quenched by addition of saturated aqueous NH₄Cl and extracted with CH₂Cl₂. The combined organic layers were washed with brine, dried over anhydrous Na₂SO₄, and concentrated *in vacuo*. The residue was purified by column chromatography (silica gel, hexanes/EtOAc, 1/1) to afford phenol **27** (25 mg, 40%): ¹H NMR (400 MHz, CDCl₃) δ 7.82–7.76 (m, 2H), 7.47 (d, *J* = 7.2 Hz, 2H), 7.37 (dd, *J* = 7.2, 7.6 Hz, 2H), 7.31 (d, *J* = 7.6 Hz, 1H), 6.89 (dd, *J* = 6.0, 8.4 Hz, 2H), 6.83 (dd, *J* = 2.0, 13.2 Hz, 2H), 6.77–6.68 (m, 3H), 5.54 (s, 1H), 5.39 (dd, *J* = 5.2, 6.0 Hz, 2H), 5.34 (dd, *J* = 4.4, 6.8 Hz, 1H), 5.18 (s, 2H), 3.93 (s, 3H), 3.89 (s, 3H), 3.84 (s, 3H), 2.24–2.20 (m, 2H), 1.64 (d, *J* = 6.8 Hz, 3H), 0.67–0.64 (m, 6H).

(R)-2-(4-[(2S,3R,4R,5S)-5-(4-[(*tert*-Butyldiphenylsilyloxy)-3-methoxyphenyl]-3,4-dimethyltetrahydrofuran-2-yl]-2-methoxyphenoxy)-1-(3-hydroxy-4-methoxyphenyl)propan-1-one (28). TBDPS Protection. To a cooled (0 °C) solution of **27** (18 mg, 0.03 mmol) in dry CH₂Cl₂ (2 mL, 0.02 M) were added imidazole (12 mg, 0.18 mmol) and TBDPSCl (0.02 mL, 0.09 mmol). After stirring for 10 h at the same temperature, the reaction was quenched by addition of saturated aqueous NH₄Cl, and the resulting mixture was extracted with CH₂Cl₂. The combined organic layers were washed with brine, dried over anhydrous Na₂SO₄, and concentrated *in vacuo*. The residue was purified by column chromatography (silica gel, hexanes/EtOAc, 3/1) to afford the corresponding ether **S2** as a white foam (24 mg, 95%): ¹H NMR (400 MHz, CDCl₃) δ 7.81–7.68 (m, 6H), 7.47–7.29 (m, 11H), 6.89 (d, *J* = 8.4 Hz, 1H), 6.82–6.66 (m, 5H), 6.53 (d, *J* = 8.4 Hz, 1H), 5.34–5.31 (m, 3H), 5.17 (s, 2H), 3.93 (s, 3H), 3.82 (s, 3H), 3.54 (s, 3H), 2.19–2.12 (m, 2H), 1.64 (d, *J* = 6.8 Hz, 3H), 1.11 (s, 9H), 0.59 (dd, *J* = 6.4, 16.0 Hz, 6H).

Bn Deprotection. To a stirred solution of **S2** (102 mg, 0.12 mmol) in EtOAc/EtOH (3/1, 12 mL, 0.1 M) was added 10% Pd/C (30 mg, 30 wt %). The resulting mixture was stirred under H₂ atmosphere at 25 °C for 8 h. The reaction mixture was then filtered through Celite with EtOAc and concentrated *in vacuo*. The residue was purified by column chromatography (silica gel, hexanes/EtOAc, 2/1) to afford phenol **28** (62 mg, 67%): ¹H NMR (400 MHz, CDCl₃) δ 7.74–7.68 (m, 6H), 7.40–7.29 (m, 6H), 6.88 (dd, *J* = 2.0, 8.4 Hz, 1H), 6.81 (dd, *J* = 2.0, 6.0 Hz, 1H), 6.75 (dd, *J* = 4.4, 8.4 Hz, 1H), 6.70–6.66 (m, 3H), 6.55–6.52 (m, 1H), 5.61 (s, 1H), 5.39 (m, 1H), 5.32 (d, *J* = 4.8 Hz, 2H), 3.95 (s, 3H), 3.84 (s, 3H), 3.54 (s, 3H), 2.18–2.12 (m, 2H), 1.68 (dd, *J* = 2.0, 6.4 Hz, 3H), 1.11 (s, 9H), 0.59 (dd, *J* = 6.4, 13.2 Hz, 6H).

MA13. To a cooled (0 °C) solution of **28** (20 mg, 0.03 mmol) in dry DMF (2 mL, 0.01 M) were added propargyl bromide (0.02 mL, 0.03 mmol) and K₂CO₃ (5.5 mg, 0.04 mmol). After stirring for 1 h at 25 °C, the reaction was quenched by addition of water, and the

resulting mixture was extracted with EtOAc. The combined organic layers were washed with brine, dried over anhydrous Na_2SO_4 , and concentrated *in vacuo*. The residue was purified by column chromatography (silica gel, hexanes/EtOAc, 2/1) to afford the corresponding ether **S3** as a white foam (14 mg, 67%): $^1\text{H NMR}$ (400 MHz, CDCl_3) δ 7.88–7.84 (m, 2H), 7.69 (dd, $J = 1.6, 8.0$ Hz, 4H), 7.40–7.30 (m, 6H), 6.90 (d, $J = 8.0$ Hz, 1H), 6.81 (dd, $J = 1.6, 9.2$ Hz, 1H), 6.77 (dd, $J = 3.6, 8.0$ Hz, 1H), 6.70–6.65 (m, 3H), 6.53 (dd, $J = 1.6, 8.4$ Hz, 1H), 5.37 (dq, $J = 4.4, 6.8$ Hz, 1H), 5.33–5.30 (m, 2H), 4.80 (d, $J = 2.4$ Hz, 2H), 3.93 (s, 3H), 3.84 (s, 3H), 3.54 (s, 3H), 2.51 (s, 1H), 2.19–2.12 (m, 2H), 1.71 (d, $J = 6.8$ Hz, 3H), 1.11 (s, 9H), 0.59 (dd, $J = 6.4, 15.6$ Hz, 6H).

TBDPS Deprotection. To a solution of **S3** (14 mg, 0.02 mmol) in dry THF (1 mL, 0.02 M) was added TBAF (1.0 M in THF, 0.04 mL, 0.04 mmol). After stirring for 5 min at 25 °C, the reaction was quenched by addition of saturated aqueous NH_4Cl , and the resulting mixture was extracted with EtOAc. The combined organic layers were washed with brine, dried over anhydrous Na_2SO_4 , and concentrated *in vacuo*. The residue was purified by column chromatography (silica gel, hexanes/EtOAc, 2/1) to afford the corresponding phenol **S4** (8 mg, 80%): $^1\text{H NMR}$ (500 MHz, CDCl_3) δ 7.79–7.84 (m, 2H), 6.92–6.68 (m, 7H), 5.52 (s, 1H), 5.40–5.36 (m, 3H), 4.81 (d, $J = 2.0$ Hz, 2H), 3.93 (s, 3H), 3.89 (s, 3H), 3.85 (s, 3H), 2.51 (s, 1H), 2.24–2.18 (m, 2H), 1.71 (d, $J = 7.0$ Hz, 3H), 0.67–0.64 (m, 6H).

Alkylation. To a cooled (0 °C) solution of **S4** (8 mg, 0.01 mmol) in dry CH_2Cl_2 (1 mL, 0.01 M) was added dropwise BEMP (0.004 mL, 0.01 mmol). The resulting mixture was stirred at the same temperature for 10 min before tosylate **26** (7 mg, 0.02 mmol) in CH_2Cl_2 (0.5 mL, 0.04 M) was added. After stirring for 30 min at 0 °C, the reaction was quenched by addition of saturated aqueous NH_4Cl , and the resulting mixture was extracted with CH_2Cl_2 . The combined organic layers were washed with brine, dried over anhydrous Na_2SO_4 , and concentrated *in vacuo*. The residue was purified by column chromatography (silica gel, hexanes/EtOAc, 2/1) to afford **MA13** as a colorless oil (5 mg, 45%): $^1\text{H NMR}$ (400 MHz, CDCl_3) δ 8.15 (dd, $J = 4.8, 8.4$ Hz, 2H), 7.88–7.84 (m, 2H), 7.23 (d, $J = 8.4$ Hz, 2H), 6.90 (d, $J = 8.4$ Hz, 1H), 6.82–6.76 (m, 4H), 6.70–6.66 (m, 2H), 5.40–5.33 (m, 4H), 4.80 (d, $J = 2.4$ Hz, 2H), 3.93 (s, 3H), 3.84 (s, 3H), 3.80 (s, 3H), 2.51 (s, 1H), 2.21–2.18 (m, 2H), 1.69 (dd, $J = 6.8, 16.0$ Hz, 6H), 0.63–0.60 (m, 6H); IR (neat) 2960, 1684, 1509, 1264, 1025 cm^{-1} ; HRMS (ESI) m/z 823.2803 [(M + Na)⁺, $\text{C}_{44}\text{H}_{43}\text{F}_3\text{N}_3\text{O}_9$ requires 823.2813].

tert-Butyl [2-(2-{2-[2-Methoxy-5-((R)-2-[2-methoxy-4-((2S,3R,4R,5S)-5-{3-methoxy-4-[(R)-1-oxo-1-[4-[3-(trifluoromethyl)-3H-diazirin-3-yl]phenyl]propan-2-yl]oxy]phenyl)-3,4-dimethyltetrahydrofuran-2-yl]phenoxy]propanoyl]phenoxy]ethoxy]ethoxy]ethyl]carbamate (29**).** **Linker Attachment.** To a solution of **28** (15 mg, 0.02 mmol) in dry DMF (2 mL, 0.01 M) was added K_2CO_3 (6 mg, 0.04 mmol) at 25 °C. After stirring for 30 min at the same temperature, the reaction mixture was cooled to 0 °C and treated with *tert*-butyl [2-[2-(2-bromoethoxy)ethoxy]ethyl]carbamate⁵⁰ (7.5 mg, 0.02 mmol) and TBAI (0.8 mg, 0.002 mmol). After stirring for 16 h at 25 °C, the reaction was quenched by addition of water, and the resulting mixture was extracted with EtOAc. The combined organic layers were washed with brine, dried over anhydrous Na_2SO_4 , and concentrated *in vacuo*. The residue was purified by column chromatography (silica gel, hexanes/EtOAc, 1/2) to afford the corresponding phenol **S5** (5 mg, 34%): $^1\text{H NMR}$ (400 MHz, CDCl_3) δ 7.82 (dd, $J = 6.0, 8.4$ Hz, 1H), 7.70 (s, 1H), 6.89–6.67 (m, 7H), 5.54 (s, 1H), 5.41–5.38 (m, 3H), 5.15 (br s, 1H), 4.23 (dd, $J = 4.8, 4.8$ Hz, 2H), 3.91–3.89 (m, 5H), 3.89 (s, 3H), 3.85 (s, 3H), 3.72 (dd, $J = 4.0, 4.8$ Hz, 2H), 3.63 (dd, $J = 4.0, 5.2$ Hz, 2H), 3.54 (dd, $J = 4.8, 5.2$ Hz, 2H), 3.31 (d, $J = 4.8$ Hz, 2H), 2.24–2.18 (m, 2H), 1.70 (d, $J = 6.8$ Hz, 3H), 1.42 (s, 9H), 0.65 (dd, $J = 6.8, 7.2$ Hz, 6H).

Alkylation. To a cooled (0 °C) solution of **S5** (24 mg, 0.03 mmol) in dry CH_2Cl_2 (2 mL, 0.02 M) was added dropwise BEMP (0.03 mL, 0.1 mmol). The resulting mixture was stirred at the same temperature for 10 min before tosylate **26** (39 mg, 0.1 mmol) in CH_2Cl_2 (1 mL, 0.1 M) was added. After stirring for 30 min at 0 °C, the reaction was quenched by addition of saturated aqueous NH_4Cl , and the resulting mixture was extracted with CH_2Cl_2 . The combined organic layers were

washed with brine, dried over anhydrous Na_2SO_4 , and concentrated *in vacuo*. The residue was purified by column chromatography (silica gel, hexanes/EtOAc, 2/1) to afford Boc-protected amine **29** (26 mg, 79%): $^1\text{H NMR}$ (400 MHz, CDCl_3) δ 8.15 (dd, $J = 4.8, 8.4$ Hz, 2H), 7.84–7.79 (m, 1H), 7.70 (s, 1H), 7.23 (d, $J = 8.4$ Hz, 2H), 6.87 (d, $J = 8.4$ Hz, 1H), 6.82–6.74 (m, 4H), 6.70–6.65 (m, 2H), 5.42–5.30 (m, 4H), 5.06 (br s, 1H), 4.23 (dd, $J = 4.8, 4.8$ Hz, 2H), 3.91–3.88 (m, 5H), 3.84 (s, 3H), 3.80 (s, 3H), 3.71 (dd, $J = 4.4, 5.2$ Hz, 2H), 3.63 (dd, $J = 4.0, 4.8$ Hz, 2H), 3.54 (dd, $J = 4.8, 5.2$ Hz, 2H), 3.31 (d, $J = 4.8$ Hz, 2H), 2.22–2.16 (m, 2H), 1.68 (dd, $J = 6.8, 10.8$ Hz, 6H), 1.41 (s, 9H), 0.63–0.59 (m, 6H).

MA14. Boc Deprotection. To a cooled (0 °C) solution of **29** (26 mg, 0.03 mmol) in dry CH_2Cl_2 (1 mL, 0.03 M) was added dropwise TFA (0.5 mL). After stirring for 40 min at the same temperature, the solvent was removed under reduced pressure. The crude residue was employed in the next step without further purification;

Biotin Attachment. The residue was dissolved in dry DMF (1 mL, 0.03 M), and the mixture was treated with Et_3N (0.009 mL, 0.06 mmol) followed by biotin *N*-hydroxysuccinimide ester (9 mg, 0.03 mmol) in DMF (1 mL, 0.03 M) at 0 °C. After stirring for 15 h at 25 °C, the reaction was quenched by addition of water, and the resulting mixture was extracted with CH_2Cl_2 . The combined organic layers were washed with brine, dried over anhydrous Na_2SO_4 , and concentrated *in vacuo*. The residue was purified by column chromatography (silica gel, $\text{CH}_2\text{Cl}_2/\text{MeOH}$, 10/1) to afford **MA14** as a colorless oil (28 mg, 99% for 2 steps): $^1\text{H NMR}$ (400 MHz, CDCl_3) δ 8.19–8.11 (m, 2H), 7.87–7.79 (m, 1H), 7.71 (s, 1H), 7.25–7.20 (m, 2H), 6.91–6.65 (m, 7H), 6.55 (br s, 1H), 5.69 (br s, 1H), 5.42–5.30 (m, 4H), 5.07–4.90 (m, 2H), 4.47–4.41 (m, 1H), 4.37–4.32 (m, 1H), 4.28–4.20 (m, 2H), 3.93–3.88 (m, 5H), 3.84 (s, 3H), 3.80 (s, 3H), 3.73–3.69 (m, 2H), 3.66–3.62 (m, 2H), 3.58–3.54 (m, 2H), 3.43–3.40 (m, 2H), 3.13–3.05 (m, 1H), 2.97–2.89 (m, 1H), 2.76–2.63 (m, 2H), 2.22–2.12 (m, 4H), 1.83–1.66 (m, 8H), 1.40–1.37 (m, 2H), 0.63–0.59 (m, 6H); IR (neat) 2162, 1506, 1148, 650 cm^{-1} ; HRMS (ESI) m/z 1120.4541 [(M + H)⁺, $\text{C}_{57}\text{H}_{68}\text{F}_3\text{N}_5\text{O}_{13}\text{S}$ requires 1120.4559].

Dual Luciferase-Reporter Assay. HEK-293T cells were seeded on 96-well plates at a density of 5×10^3 cells/well and allowed to attach for 24 h. Cells were transfected with pGL3-SHRE-VEGF-luciferase plasmid containing five copies of HREs in human VEGF promoter and pRL-SV40 plasmid encoding *Renilla* luciferase using Vivamagic transfection reagent (Vivagene, Seongnam, Korea), according to the manufacturer's instructions. Cells were treated with hypoxic conditions (1% O_2) and serially diluted compounds for 24 h after transfection. Luciferase reporter assay was performed using the Dual-Glo luciferase assay system (Promega, Madison, WI, USA) according to the manufacturer's instructions. Briefly, an equal volume of Dual-Glo reagent to culture medium was added to each well, and the mixture was incubated for 10 min. The firefly luminescence was measured using a microplate reader (Infinite M200 Pro, TECAN, Männedorf, Switzerland). Dual-Glo Stop & Glo reagent was added, and the mixture was incubated for 10 min before the measurement of *Renilla* luminescence. The firefly luminescence signals were normalized to the activity of *Renilla* luciferase. Three independent experiments were performed.

MTT Assay. Cells were seeded on 96-well plates at a density of 1×10^4 cells/well, and then incubated for 24 h. After cells were treated with various concentrations of compounds for 24 h under hypoxia, 3-(4,5-dimethylthiazol-2-yl)-2,5-diphenyltetrazolium bromide (MTT, AMRESCO) solution was added to each well, and the mixture was incubated for another 4 h at 37 °C. The resulting formazan crystals were dissolved in DMSO (100 μL /well) and the absorbance of the plate was read with a microplate reader (Infinite M200 Pro, TECAN, Männedorf, Switzerland) at 540 nm. Three independent experiments were performed.

Western Blot Analysis. Proteins were extracted from the cells using PRO-PREP (iNtRon Biotech, South Korea). Cell extracts were separated by SDS-PAGE and transferred to a nitrocellulose membrane (Whatman, Maidstone, England). The membranes were blocked with 5% skim milk in Tris-buffered saline (TBS) containing 0.1% Tween-20 for 30 min at room temperature. After blocking, membranes were

incubated with specific primary antibodies overnight at 4 °C, followed by incubation with horseradish peroxidase-conjugated mouse- or rabbit-IgG for 1 h at room temperature. Membranes were then incubated with horseradish peroxidase-conjugated antibody mouse or rabbit immunoglobulins at room temperature and developed through West Pico chemiluminescent substrate (Pierce, Woburn, MA, USA).

RNA Isolation, Reverse Transcription–Polymerase Chain Reaction (RT-PCR). Total RNA was extracted from cells using TRIzol Reagent (Invitrogen, Carlsbad, CA), and cDNA synthesis was performed using MMLV reverse transcriptase. Real-time PCR was performed using a SYBR Green PCR Master Mix (Applied Biosystems, CA, USA). Each PCR reaction contained cDNA with 10-fold dilution and gene-specific primers. The thermal cycle used was 2 min at 50 °C, 10 min at 95 °C, 40 cycles of 15 s denaturation at 95 °C with 1 min annealing at 60 °C. The mean cycle threshold (CT) values were calculated for the gene expression with normalization to β -actin as an internal control. Each experiment was performed in triplicate, and the average was calculated.

■ ASSOCIATED CONTENT

■ Supporting Information

The Supporting Information is available free of charge on the ACS Publications website at DOI: 10.1021/acs.jmedchem.5b01220.

Dual luciferase-reporter assay data, MTT assay data, NCI 60-cell line screen data, calculation of physicochemical properties, and copies ¹H and ¹³C NMR spectra (PDF) Table of SMILES representations and IC₅₀ values (CSV)

■ AUTHOR INFORMATION

Corresponding Authors

*You Mie Lee, Ph.D. E-mail: lym@knu.ac.kr. Telephone: 82-53-950-8566. Fax: 82-53-950-8557.

*Jiyong Hong, Ph.D. E-mail: jiyong.hong@duke.edu. Telephone: 1-919-660-1545. Fax: 1-919-660-1605.

Author Contributions

#D.-Y.K. and H.E.L. contributed equally.

Notes

The authors declare no competing financial interest.

■ ACKNOWLEDGMENTS

We are grateful to Dr. Sung Hee Park for assistance with luciferase data analysis and to NCI DTP for the NCI 60-cell line screen data (Supporting Information). We are grateful to the American Cancer Society (Grant 122057-RSG-12-045-01-CDD to J.H.), the National Research Foundation (MSIP, Korea, Grant NRF-2012R1A4A1028835 to Y.M.L.), the National Institutes of Health/Duke Cancer Institute (Grant P30 CA014236 to J.H.), and the Alexander and Margaret Stewart Trust (J.H.) for funding this work. We also thank the North Carolina Biotechnology Center (NCBC; Grant No. 2008-IDG-1010) for funding of the NMR instrumentation and the National Science Foundation (NSF) MRI Program (Award ID No. 0923097) for funding mass spectrometry instrumentation. T.N.S. was supported by the NSF Graduate Research Fellowship Program.

■ ABBREVIATIONS USED

BEI, binding efficiency index; BEMP, 2-tert-butylimino-2-diethylamino-1,3-dimethylperhydro-1,3,2-diazaphosphorine; brsm, based on recovered starting material; Cdk, cyclin-dependent kinase; DDQ, 2,3-dichloro-5,6-dicyano-1,4-benzoquinone; HIF-1, hypoxia-inducible factor; HRE, hypoxia

response element; LE, ligand efficiency; LEI, ligand efficiency index; MTT, 3-(4,5-dimethylthiazol-2-yl)-2,5-diphenyltetrazolium bromide; ODD, oxygen-dependent degradation; PD, pharmacodynamic; PHD, prolyl hydroxylase domain; PK, pharmacokinetic; RLU, relative light units; SAR, structure–activity relationship; VEGF, vascular endothelial growth factor; VHL, von Hippel–Lindau

■ REFERENCES

- (1) Semenza, G. L. Targeting HIF-1 for cancer therapy. *Nat. Rev. Cancer* **2003**, *3*, 721–732.
- (2) Bertout, J. A.; Patel, S. A.; Simon, M. C. The impact of O₂ availability on human cancer. *Nat. Rev. Cancer* **2008**, *8*, 967–975.
- (3) Semenza, G. L. Oxygen sensing, hypoxia-inducible factors, and disease pathophysiology. *Annu. Rev. Pathol.: Mech. Dis.* **2014**, *9*, 47–71.
- (4) Wang, G. L.; Jiang, B. H.; Rue, E. A.; Semenza, G. L. Hypoxia-inducible factor 1 is a basic-helix-loop-helix-PAS heterodimer regulated by cellular O₂ tension. *Proc. Natl. Acad. Sci. U. S. A.* **1995**, *92*, 5510–5514.
- (5) Bruck, R. K.; McKnight, S. L. A conserved family of prolyl-4-hydroxylases that modify HIF. *Science* **2001**, *294*, 1337–1340.
- (6) Semenza, G. L. Hydroxylation of HIF-1: oxygen sensing at the molecular level. *News Physiol. Sci.* **2004**, *19*, 176–182.
- (7) Lisy, K.; Peet, D. J. Turn me on: regulating HIF transcriptional activity. *Cell Death Differ.* **2008**, *15*, 642–649.
- (8) Vaupel, P. Tumor microenvironmental physiology and its implications for radiation oncology. *Semin. Radiat. Oncol.* **2004**, *14*, 198–206.
- (9) Brizel, D. M.; Sibley, G. S.; Prosnitz, L. R.; Scher, R. L.; Dewhirst, M. W. Tumor hypoxia adversely affects the prognosis of carcinoma of the head and neck. *Int. J. Radiat. Oncol., Biol., Phys.* **1997**, *38*, 285–289.
- (10) Hockel, M.; Schlenger, K.; Aral, B.; Mitze, M.; Schaffer, U.; Vaupel, P. Association between tumor hypoxia and malignant progression in advanced cancer of the uterine cervix. *Cancer Res.* **1996**, *56*, 4509–4515.
- (11) Moon, E. J.; Brizel, D. M.; Chi, J. T.; Dewhirst, M. W. The potential role of intrinsic hypoxia markers as prognostic variables in cancer. *Antioxid. Redox Signaling* **2007**, *9*, 1237–1294.
- (12) Semenza, G. L. Evaluation of HIF-1 inhibitors as anticancer agents. *Drug Discovery Today* **2007**, *12*, 853–859.
- (13) Aebbersold, D. M.; Burri, P.; Beer, K. T.; Laissue, J.; Djonov, V.; Greiner, R. H.; Semenza, G. L. Expression of hypoxia-inducible factor-1 α : a novel predictive and prognostic parameter in the radiotherapy of oropharyngeal cancer. *Cancer Res.* **2001**, *61*, 2911–2916.
- (14) Moeller, B. J.; Cao, Y.; Li, C. Y.; Dewhirst, M. W. Radiation activates HIF-1 to regulate vascular radiosensitivity in tumors: role of reoxygenation, free radicals, and stress granules. *Cancer Cell* **2004**, *5*, 429–441.
- (15) Koukourakis, M. I.; Giatromanolaki, A.; Sivridis, E.; Simopoulos, C.; Turlay, H.; Talks, K.; Gatter, K. C.; Harris, A. L. Hypoxia-inducible factor (HIF1A and HIF2A), angiogenesis, and chemoradiotherapy outcome of squamous cell head-and-neck cancer. *Int. J. Radiat. Oncol., Biol., Phys.* **2002**, *53*, 1192–1202.
- (16) Giaccia, A.; Siim, B. G.; Johnson, R. S. HIF-1 as a target for drug development. *Nat. Rev. Drug Discovery* **2003**, *2*, 803–811.
- (17) Lin, X.; David, C. A.; Donnelly, J. B.; Michaelides, M.; Chandel, N. S.; Huang, X.; Warrior, U.; Weinberg, F.; Tormos, K. V.; Fesik, S. W.; Shen, Y. A chemical genomics screen highlights the essential role of mitochondria in HIF-1 regulation. *Proc. Natl. Acad. Sci. U. S. A.* **2008**, *105*, 174–179.
- (18) Zhang, H.; Qian, D. Z.; Tan, Y. S.; Lee, K.; Gao, P.; Ren, Y. R.; Rey, S.; Hammers, H.; Chang, D.; Pili, R.; Dang, C. V.; Liu, J. O.; Semenza, G. L. Digoxin and other cardiac glycosides inhibit HIF-1 α synthesis and block tumor growth. *Proc. Natl. Acad. Sci. U. S. A.* **2008**, *105*, 19579–19586.
- (19) Ellinghaus, P.; Heisler, I.; Unterschemmann, K.; Haerter, M.; Beck, H.; Greschat, S.; Ehrmann, A.; Summer, H.; Flamme, I.; Oehme,

F.; Thierauch, K.; Michels, M.; Hess-Stumpp, H.; Ziegelbauer, K. BAY 87–2243, a highly potent and selective inhibitor of hypoxia-induced gene activation has antitumor activities by inhibition of mitochondrial complex I. *Cancer Med.* **2013**, *2*, 611–624.

(20) Lee, K.; Kang, J. E.; Park, S.-K.; Jin, Y.; Chung, K.-S.; Kim, H.-M.; Lee, K.; Kang, M. R.; Lee, M. K.; Song, K. B.; Yang, E.-G.; Lee, J.-J.; Won, M. LW6, a novel HIF-1 inhibitor, promotes proteasomal degradation of HIF-1 α via upregulation of VHL in a colon cancer cell line. *Biochem. Pharmacol.* **2010**, *80*, 982–989.

(21) Rao, K. V.; Alvarez, F. M. Manassantins A/B and Saucerneol - novel biologically-active lignoids from *Saururus cernuus*. *Tetrahedron Lett.* **1983**, *24*, 4947–4950.

(22) Hodges, T. W.; Hossain, C. F.; Kim, Y. P.; Zhou, Y. D.; Nagle, D. G. Molecular-targeted antitumor agents: the *Saururus cernuus* dineolignans manassantin B and 4-O-demethylmanassantin B are potent inhibitors of hypoxia-activated HIF-1. *J. Nat. Prod.* **2004**, *67*, 767–771.

(23) Hossain, C. F.; Kim, Y. P.; Baerson, S. R.; Zhang, L.; Bruick, R. K.; Mohammed, K. A.; Agarwal, A. K.; Nagle, D. G.; Zhou, Y. D. *Saururus cernuus* lignans - potent small molecule inhibitors of hypoxia-inducible factor-1. *Biochem. Biophys. Res. Commun.* **2005**, *333*, 1026–1033.

(24) Kim, H.; Kasper, A. C.; Moon, E. J.; Park, Y.; Wooten, C. M.; Dewhirst, M. W.; Hong, J. Nucleophilic addition of organozinc reagents to 2-sulfonyl cyclic ethers: stereoselective synthesis of manassantins A and B. *Org. Lett.* **2009**, *11*, 89–92.

(25) Hong, J. Role of natural product diversity in chemical biology. *Curr. Opin. Chem. Biol.* **2011**, *15*, 350–354.

(26) Hong, J. Natural product synthesis at the interface of chemistry and biology. *Chem. - Eur. J.* **2014**, *20*, 10204–10212.

(27) Kim, H.; Baker, J. B.; Lee, S. U.; Park, Y.; Bolduc, K. L.; Park, H. B.; Dickens, M. G.; Lee, D. S.; Kim, Y.; Kim, S. H.; Hong, J. Stereoselective synthesis and osteogenic activity of subglutinols A and B. *J. Am. Chem. Soc.* **2009**, *131*, 3192–3194.

(28) Ying, Y.; Taori, K.; Kim, H.; Hong, J.; Luesch, H. Total synthesis and molecular target of largazole, a histone deacetylase inhibitor. *J. Am. Chem. Soc.* **2008**, *130*, 8455–8459.

(29) Kasper, A. C.; Moon, E. J.; Hu, X.; Park, Y.; Wooten, C. M.; Kim, H.; Yang, W.; Dewhirst, M. W.; Hong, J. Analysis of HIF-1 inhibition by manassantin A and analogues with modified tetrahydrofuran configurations. *Bioorg. Med. Chem. Lett.* **2009**, *19*, 3783–3786.

(30) Shoemaker, R. H. The NCI60 human tumour cell line anticancer drug screen. *Nat. Rev. Cancer* **2006**, *6*, 813–823.

(31) Qu, M.-N.; Zhou, L.; Cao, X.-P. First synthesis of a series of new natural glucosides. *Chin. J. Chem.* **2006**, *24*, 1625–1630.

(32) Kolb, H. C.; Vannieuwenhze, M. S.; Sharpless, K. B. Catalytic asymmetric dihydroxylation. *Chem. Rev.* **1994**, *94*, 2483–2547.

(33) Moreno, I.; Tellitu, I.; Dominguez, E.; SanMartin, R. A simple route to new phenanthro- and phenanthroid-fused thiazoles by a PIFA-mediated (hetero)biaryl coupling reaction. *Eur. J. Org. Chem.* **2002**, 2126–2135.

(34) Corey, E. J.; Bakshi, R. K.; Shibata, S. Highly enantioselective borane reduction of ketones catalyzed by chiral oxazaborolidines - mechanism and synthetic implications. *J. Am. Chem. Soc.* **1987**, *109*, 5551–5553.

(35) Kerns, E. H.; Di, L. *Drug-like Properties: Concepts, Structure Design and Methods: From ADME to Toxicity Optimization*; Academic Press: Amsterdam; Boston, 2008.

(36) Hopkins, A. L.; Keseru, G. M.; Leeson, P. D.; Rees, D. C.; Reynolds, C. H. The role of ligand efficiency metrics in drug discovery. *Nat. Rev. Drug Discovery* **2014**, *13*, 105–121.

(37) Abad-Zapatero, C.; Metz, J. T. Ligand efficiency indices as guideposts for drug discovery. *Drug Discovery Today* **2005**, *10*, 464–469.

(38) Zanger, U. M.; Schwab, M. Cytochrome P450 enzymes in drug metabolism: Regulation of gene expression, enzyme activities, and impact of genetic variation. *Pharmacol. Ther.* **2013**, *138*, 103–141.

(39) Yu, M. J.; Zheng, W.; Seletsky, B. M. From micrograms to grams: Scale-up synthesis of eribulin mesylate. *Nat. Prod. Rep.* **2013**, *30*, 1158–1164.

(40) Kasper, A. C.; Baker, J. B.; Kim, H.; Hong, J. The end game of chemical genetics: target identification. *Future Med. Chem.* **2009**, *1*, 727–736.

(41) Sakamoto, S.; Hatakeyama, M.; Ito, T.; Handa, H. Tools and methodologies capable of isolating and identifying a target molecule for a bioactive compound. *Bioorg. Med. Chem.* **2012**, *20*, 1990–2001.

(42) Taunton, J.; Hassig, C. A.; Schreiber, S. L. A mammalian histone deacetylase related to the yeast transcriptional regulator Rpd3p. *Science* **1996**, *272*, 408–411.

(43) Kotake, Y.; Sagane, K.; Owa, T.; Mimori-Kiyosue, Y.; Shimizu, H.; Uesugi, M.; Ishihama, Y.; Iwata, M.; Mizui, Y. Splicing factor SF3b as a target of the antitumor natural product pladienolide. *Nat. Chem. Biol.* **2007**, *3*, 570–575.

(44) Tomohiro, T.; Hashimoto, M.; Hatanaka, Y. Cross-linking chemistry and biology: development of multifunctional photoaffinity probes. *Chem. Rec.* **2005**, *5*, 385–395.

(45) Subramanian, A.; Tamayo, P.; Mootha, V. K.; Mukherjee, S.; Ebert, B. L.; Gillette, M. A.; Paulovich, A.; Pomeroy, S. L.; Golub, T. R.; Lander, E. S.; Mesirov, J. P. Gene set enrichment analysis: a knowledge-based approach for interpreting genome-wide expression profiles. *Proc. Natl. Acad. Sci. U. S. A.* **2005**, *102*, 15545–15550.

(46) Bild, A. H.; Yao, G.; Chang, J. T.; Wang, Q.; Potti, A.; Chasse, D.; Joshi, M. B.; Harpole, D.; Lancaster, J. M.; Berchuck, A.; Olson, J. A., Jr.; Marks, J. R.; Dressman, H. K.; West, M.; Nevins, J. R. Oncogenic pathway signatures in human cancers as a guide to targeted therapies. *Nature* **2006**, *439*, 353–357.

(47) West, G. M.; Tucker, C. L.; Xu, T.; Park, S. K.; Han, X.; Yates, J. R., 3rd; Fitzgerald, M. C. Quantitative proteomics approach for identifying protein-drug interactions in complex mixtures using protein stability measurements. *Proc. Natl. Acad. Sci. U. S. A.* **2010**, *107*, 9078–9082.

(48) Strickland, E. C.; Geer, M. A.; Tran, D. T.; Adhikari, J.; West, G. M.; DeArmond, P. D.; Xu, Y.; Fitzgerald, M. C. Thermodynamic analysis of protein-ligand binding interactions in complex biological mixtures using the stability of proteins from rates of oxidation. *Nat. Protoc.* **2013**, *8*, 148–161.

(49) McGuigan, C.; Bidet, O.; Derudas, M.; Andrei, G.; Snoeck, R.; Balzarini, J. Alkenyl substituted bicyclic nucleoside analogues retain nanomolar potency against Varicella Zoster Virus. *Bioorg. Med. Chem.* **2009**, *17*, 3025–3027.

(50) Hatanaka, Y.; Hashimoto, M.; Kanaoka, Y. A novel biotinylated heterobifunctional cross-linking reagent bearing an aromatic diazirine. *Bioorg. Med. Chem.* **1994**, *2*, 1367–1373.